© 2022. Published by The Company of Biologists Ltd | Journal of Experimental Biology (2022) 225, jeb242795. doi:10.1242/jeb.242795

RESEARCH ARTICLE

Terrestrial force production by the limbs of a semi-aquatic salamander provides insight into the evolution of terrestrial locomotor mechanics

Sandy M. Kawano[1,*] and Richard W. Blob[2]

ABSTRACT

Amphibious fishes and salamanders are valuable functional analogs for vertebrates that spanned the water–land transition. However, investigations of walking mechanics have focused on terrestrial salamanders and, thus, may better reflect the capabilities of stem tetrapods that were already terrestrial. The earliest tetrapods were likely aquatic, so salamanders that are not primarily terrestrial may yield more appropriate data for modeling the incipient stages of terrestrial locomotion. In the present study, locomotor biomechanics were quantified from semi-aquatic *Pleurodeles waltl*, a salamander that spends most of its adult life in water, and then compared with those of a primarily terrestrial salamander (*Ambystoma tigrinum*) and a semi-aquatic fish (*Periophthalmus barbarus*) to evaluate whether terrestrial locomotion was more comparable between species with ecological versus phylogenetic similarities. Ground reaction forces (GRFs) from individual limbs or fins indicated that the pectoral appendages of each taxon had distinct patterns of force production, but GRFs from the hindlimbs were comparable between the salamander species. The rate at which force is produced can affect musculoskeletal function, so we also calculated 'yank' (first time derivative of force) to quantify the dynamics of GRF production. Yank was sometimes slower in *P. waltl* but there were some similarities between the three species. Finally, the semi-aquatic taxa (*P. waltl* and *P. barbarus*) had a more medial inclination of the GRF compared to terrestrial salamanders, potentially elevating bone stresses among more aquatic taxa and limiting their excursions onto land.

KEY WORDS: Biomechanics, Ground reaction force, Terrestrial locomotion, Salamander, Fish, Yank

INTRODUCTION

The evolutionary invasion of land was a seminal event in vertebrate history that has received intense study, with integrative approaches filling major gaps in our understanding of how this transition transpired (Ashley-Ross et al., 2013; Molnar et al., 2021). Skeletal remains and trackways in the fossil record can provide some of the most direct evidence about morphological transformations and gait patterns, respectively, as vertebrates became terrestrial (Ahlberg, 2018), yet also present general challenges given the limits to which fossils preserve biomechanical parameters, such as muscle leverage (Molnar et al., 2021) and bone loading (Hohn-Schulte et al., 2013), that are often simulated or validated based on empirical data from living taxa. Consequently, extant amphibious fishes, amphibians and reptiles have been used as functional models to infer the biology of extinct tetrapodomorphs (tetrapods and tetrapod-like sarcopterygian fishes) (Nyakatura et al., 2014; Nyakatura et al., 2019; Pierce et al., 2013), with extant taxa representing alternative strategies for invading land and potentially serving as models for different functional stages as vertebrates became terrestrial. Investigations of extant taxa exhibiting morphological and/or behavioral traits that are consistent with those of extinct tetrapodomorphs offer particularly intriguing opportunities to evaluate how tetrapods might have left the water's edge (Molnar et al., 2021; Pierce et al., 2013).

In considerations of locomotor performance during the invasion of land, salamanders are often used as functional analogs for early tetrapods as they move between water and land (Karakasiliotis et al., 2012), and exhibit a relatively generalized tetrapod Bauplan that has not changed substantially for at least 150 million years (Gao and Shubin, 2001) and possibly as long as 230 million years (Schoch et al., 2020). Living salamanders have been used to study the *in vivo* biomechanics and muscle physiology of walking underwater (Ashley-Ross et al., 2009; Azizi and Horton, 2004; Deban and Schilling, 2009; Frolich and Biewener, 1992), walking on land (Ashley-Ross et al., 2009; Brand, 1996; Deban and Schilling, 2009; Delvolvé et al., 1997; Frolich and Biewener, 1992; Kawano and Blob, 2013; Pierce et al., 2020; Sheffield and Blob, 2011) and transitioning between water and land (Ashley-Ross and Bechtel, 2004). However, the extant salamanders that have traditionally been studied in this context [e.g. *Ambystoma* (Sheffield and Blob, 2011), *Salamandra* (Pierce et al., 2020) and *Dicamptodon* (Ashley-Ross, 1994)] have typically been highly terrestrial (following ecological classifications from Fabre et al., 2020). For instance, *Ambystoma tigrinum* are found in various terrestrial habitats, ranging from conifer forests to deserts, and adults rarely spend extended durations in water for reasons other than reproduction (Petranka, 1998). Consequently, existing literature on the locomotor biomechanics of salamanders may reflect a biased sample that does not consider the continuum from aquatic to terrestrial habitats.

Given the greater effect of gravitational loads on the musculoskeletal system in terrestrial environments (Young et al., 2017), one of the most fundamental requirements for moving on land is the ability to support body weight for maintaining posture and generating the physical forces for locomotion. Locomotor kinetics of individual limbs during terrestrial locomotion have been assessed through measurements of ground reaction forces (GRFs) in the tiger salamander, *A. tigrinum*, and demonstrated that the hindlimbs support a similar proportion of body weight to the forelimbs but have a greater contribution to acceleration (Kawano and Blob, 2013). Moreover, force plate analyses demonstrated that

[1]Department of Biological Sciences, The George Washington University, Washington, DC 20052, USA. [2]Department of Biological Sciences, Clemson University, Clemson, SC 29634, USA.

*Author for correspondence (smkawano@gwu.edu)

S.M.K., 0000-0002-1856-5566; R.W.B., 0000-0001-5026-343X

Received 1 May 2021; Accepted 4 March 2022

Journal of Experimental Biology (2022) 225, jeb242795. doi:10.1242/jeb.242795

tiger salamanders and tuataras use inverted pendulum mechanics to recover mechanical energy during walking and running (Reilly et al., 2006), which would benefit terrestrial invaders by reducing the costs of locomotion on land. However, it is unclear whether these patterns are consistent across salamanders that spend less time on land as adults. Additional studies that compare salamanders with different terrestrial capabilities could provide insight into whether terrestrial species exhibit traits that would improve their locomotor biomechanics on land.

Because salamanders have a diverse range of habitat preferences and life histories (Wake, 2009), they provide an opportunity to compare the locomotor biomechanics of species that spend different proportions of time in aquatic versus terrestrial environments. The Spanish ribbed newt, *Pleurodeles waltl* Michahelles 1830, is one of the largest salamanders that spends a greater proportion of its life cycle living in water (Obst et al., 1988) compared with more commonly studied (terrestrial) salamanders, yet still normally makes terrestrial excursions (Fig. 1) (Karakasiliotis et al., 2012). Previous studies on the muscle activity (Delvolvé et al., 1997), bone microanatomy (Canoville and Laurin, 2009; Laurin et al., 2004) and kinematics and morphology (Karakasiliotis et al., 2012) of *P. waltl* provide a foundation for comparisons with data from more commonly studied terrestrial ambystomatid salamanders (Ashley-Ross and Barker, 2002; Bennett et al., 1989; Deban and Schilling, 2009; Kawano and Blob, 2013; Laurin et al., 2004; Stokely and Holle, 1954). Thus, GRF data from the semi-aquatic *P. waltl* and more terrestrial taxa (e.g. *A. tigrinum*) can be used to evaluate whether limb function differs between salamanders that have different propensities to move on land.

Propulsion driven primarily by the hindlimbs (‘rear-wheel drive’) occurs during terrestrial locomotion in salamanders (Kawano and Blob, 2013), and may have originally evolved for aquatic locomotion when vertebrates were still fully aquatic (King et al., 2011). However, terrestrial propulsion in early stem tetrapods may have initially been dominated by the forelimb (‘front-wheel drive’), with the transition to hindlimb dominance (‘rear-wheel drive’) only occurring later in the water–land transition as the hindlimbs assumed a more important locomotor role (Boisvert, 2005; Molnar et al., 2020). The ‘front-wheel drive’ strategy proposed for the sarcopterygian fish *Panderichthys* (Boisvert, 2005) and the early tetrapod *Ichthyostega* (Pierce et al., 2012) might be appropriately modeled by extant amphibious fishes (i.e. *Clarias* catfish and mudskippers, respectively) whose pectoral fins are used for terrestrial excursions while the pelvic fins are not (Kawano and Blob, 2013; Pace and Gibb, 2014). In contrast, the ‘rear-wheel drive’ of more crownward early tetrapods might be better modeled using terrestrial salamanders (Pierce et al., 2013), such as *A. tigrinum*. Our past work showed distinct GRF patterns between these groups, with those produced by the pectoral fins of mudskippers directed more medially (∼17 deg) than those produced by the limbs of terrestrial salamanders, or almost any other terrestrial tetrapod (generally less than 11 deg) (Kawano and Blob, 2013). Such differences could have substantial implications for the stresses experienced by the limb bones by increasing moment arms of the GRFs that contribute to bending, which could make bones more vulnerable to fracture. However, it is unclear whether a salamander with lower terrestrial capabilities would have GRF patterns that are intermediate between those of the mudskipper fish and terrestrial salamanders, and in what ways the mechanisms that generate the GRF patterns differ across appendages.

In this study, we compared the kinetics of terrestrial locomotion in amphibious fish and salamanders to gain a better understanding of how locomotor biomechanics differ between fins and limbs. First, we compared GRFs of individual limbs produced by semi-aquatic salamanders (Spanish ribbed newts, *P. waltl*) with published data on terrestrial tiger salamanders, *Ambystoma tigrinum* Green 1825, and semi-aquatic African mudskippers, *Periophthalmus barbarus* (Linnaeus 1766) (Kawano and Blob, 2013). GRF data provide information about propulsion, maneuverability and stability, and represent the external forces that are loaded upon the bones as a result of making contact with the substrate. While peak force magnitudes have been commonly used to model peak stresses to the limb bones during terrestrial locomotion (Blob, 2001), rates of loading help trigger bone remodeling (Aiello et al., 2015). Thus, we also quantified the dynamics of external force development through calculation of ‘yank’, which represents the first time derivative of force (*sensu* Lin et al., 2019). When evaluated at the organismal level, yank is measured as the rate of change in GRF. Positive and negative yank values would indicate that the rate of force production was increasing or decreasing, respectively. Yank has important implications for musculoskeletal function but was only recently defined formally, providing a promising avenue for future research on locomotor biomechanics.

Lin and colleagues (2019) presented case studies to highlight how yank measures can help explain dynamics in biological motor and sensorimotor feedback systems. Extending these analyses to a wider range of taxa (e.g. fishes and salamanders) may lend new perspectives on broadscale patterns of dynamic locomotor forces within and across taxa with diverse musculoskeletal designs. Yank

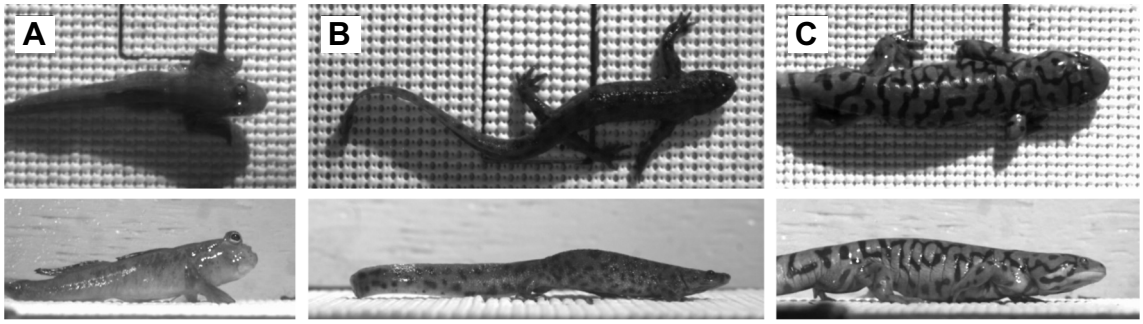

Fig. 1. The study species, walking on a force plate. Dorsal view (top row; filmed through a mirror) and lateral view (bottom row) of (A) a semi-aquatic African mudskipper (*Periophthalmus barbarus*), (B) a semi-aquatic Spanish ribbed newt (*Pleurodeles waltl*) and (C) a primarily terrestrial tiger salamander (*Ambystoma tigrinum*) walking on a force plate. Still images from the representative videos depict *P. waltl* and *A. tigrinum* using a diagonal couplet walking gait involving lateral undulations of the trunk while they walked in a straight path across the force plate, and *P. barbarus* ‘crutching’ in a straight line while keeping the body axis straight. *Pleurodeles waltl* and *P. barbarus* achieve more extended joint angles in their appendages compared with *A. tigrinum*.

was demonstrated to be an important measure for rapid movements such as jumping, where maximum take-off velocity is related to locomotor performance. Using a computer simulation, Lin and colleagues (2019) found that increasing yank decreased the time to take-off and increased jump velocity. Jumping animals can exhibit a trade-off between time-limited, submaximal force production (i.e. bullfrogs) versus non-time-limited, maximal muscle contraction (i.e. grasshoppers) (Rosario et al., 2016). Findings from the computational model led Lin and colleagues (2019) to propose yank as a mechanism to avoid the trade-off between reduced contact time versus faster take-off velocities. Yank can also be relevant to movements that are less time limited, such as sensory responses to environmental stimuli. For instance, Golgi tendon organs (GTOs) are distributed across the muscle–tendon junctions of vertebrates, respond to changes in muscle forces, and are primarily found in the skeletal muscles of tachymetabolic tetrapods (birds and mammals) versus in the tendons of bradymetabolic tetrapods (amphibians, lizards, turtles, crocodilians) (Granatosky et al., 2020). Differences in the functional morphology of GTOs allow tachymetabolic tetrapods to have more fine-scale resolution of internal force changes within muscles, compared with bradymetabolic tetrapods that would only detect coarse-scale force changes across the entire muscle, and more predictable loading regimes upon the hindlimbs that would reduce the metabolic costs of locomotion (Granatosky et al., 2020). Moreover, cursorial mammals, salamanders and tuataras exhibit comparable pendular mechanics but the last two taxa tend to exhibit larger changes in vertical displacement (i.e. potential energy) compared with mammals, which may be a plesiomorphic condition for tetrapod locomotion (Reilly et al., 2006). As a result, non-tachymetabolic taxa may exhibit larger yank magnitudes that reflect their variable locomotor mechanics and loading. Consequently, expanding yank analyses to salamanders and fishes may reveal how the dynamics of motor systems vary in taxa with more variable bone loading than mammals and birds, and shed light on the evolution of terrestrial locomotion in vertebrates.

Our data from semi-aquatic *P. waltl* can give new insights into the functional differences between fins and limbs during terrestrial locomotion in taxa that exhibit a range of terrestrial capabilities. Simply by having limbs, *P. waltl* locomotor force production may be similar to that of terrestrial salamanders such as adult *A. tigrinum*. However, the habitual use of the limbs for aquatic locomotion by adult *P. waltl* might lead to kinetic similarities with other semi-aquatic taxa, such as mudskipper fish. These comparisons carry broader implications for generating hypotheses about the emergence of functional disparity between locomotor structures, such as whether changes in functional performance are coupled across major structural changes (e.g. transition from fin to limb) or through gradual steps related to loading regimes that are potentially decoupled from structural changes (e.g. the transition from aquatic to terrestrial habitats, regardless of which locomotor structure is used).

MATERIALS AND METHODS

Animals

Five adult *P. waltl* (body mass: 16.60±0.40 g; snout–vent length: 0.083±0.001 m; total length: 0.186±0.003 m) were obtained from a commercial vendor. All values represent means±1 s.e.m. Animals were individually housed in glass aquaria that were aerated with sponge filters, kept on a 12 h:12 h light:dark cycle, and fed every 1–2 days on a diet of defrosted bloodworms and krill. Prior to testing, animals were starved for 2 days to reduce the effects of satiation on locomotor performance (Sass and Motta, 2002). Experimental and animal care procedures were approved by the Institutional Animal Care and Use Committee at Clemson University (protocols 2009-071, 2010-066).

Collection of 3D ground reaction forces

Experimental procedures from a previous study on the GRFs of tiger salamanders and mudskipper fish (Kawano and Blob, 2013) were replicated in the present study (see 'Criteria for selecting trials for GRF measurements' and 'Experimental procedures' in Supplementary Materials and Methods) to obtain forelimb (n=50) and hindlimb (n=49) GRFs from *P. waltl* (Fig. 1). Custom code to replicate these analyses is available from GitHub (https://github.com/MorphoFun/kraken). The focal taxa examined in the present study represent models for distinct functional stages during the evolution of terrestrial locomotion: front-wheel drive in a semi-aquatic vertebrate (semi-aquatic mudskipper *P. barbarus* fish), a semi-aquatic vertebrate with a generalized tetrapod Bauplan that has yet to be confirmed as being front-wheel or rear-wheel driven (semi-aquatic *P. waltl* salamander), and rear-wheel drive in a terrestrial vertebrate with a generalized tetrapod Bauplan (terrestrial *A. tigrinum* salamander). Baseline data collected from the force plate were zeroed at the beginning of each trial, when no structures had recently contacted the force plate. GRFs in the vertical, mediolateral and anteroposterior directions were digitally filtered with a custom low-pass, zero-phase second-order Butterworth filter, and then interpolated to 101 points (0–100% of stance at 1% increments) using a cubic spline with the *signal* R package (https://CRAN.R-project.org/package=signal). The stance phase was defined to begin at the first video frame when the entire foot was flat against the ground, and to end at the frame penultimate to the beginning of the swing phase.

Interspecific and intraspecific comparisons were made between fins and limbs. First, GRFs from the forelimbs and hindlimbs of *P. waltl* were compared with published data from the pectoral and pelvic appendages of mudskipper fish and tiger salamanders (Kawano and Blob, 2013) to assess whether the kinetics of semi-aquatic salamander limbs were more similar to those of mudskipper pectoral fins or terrestrial salamander limbs. Second, GRFs were compared between the forelimbs and hindlimbs for *P. waltl* to determine whether this species used forelimb-driven or hindlimb-driven propulsion. Third, GRF data from these three species were used to conduct new analyses of yank (*sensu* Lin et al., 2019) to quantify the rate of change in the GRFs produced by fins versus limbs. Linear mixed effects models (LMMs) were used to compare magnitudes and angles of orientation of GRFs when forces were maximal ('peak net GRF'), and the range of yank values between the species and appendages (see 'Statistical analyses', below).

Statistical analyses

LMMs with random intercepts via the *lme4* package (Bates et al., 2015) were used to compare the biomechanical variables of interest while accounting for the non-independence of multiple trials sampled per individual, and fitted with restricted maximum likelihood (REML) to produce unbiased estimates. All analyses were conducted in *R* version 3.6.1 (http://www.R-project.org/) and *RStudio* version 1.2.1335 (http://www.rstudio.com/). LMMs were conducted to account for the non-independence caused by trials being nested within individuals and the unequal sample sizes across individuals (for additional information, see 'Details on statistical analyses' in Supplementary Materials and Methods). LMMs also have the advantage that they do not make assumptions about balanced designs, homogeneity of variance, etc., so the model assumptions only include random sampling and normality of the residuals (reviewed in Smith, 2017). Evaluation of quantile–quantile (Q–Q)

plots indicated that there were no major deviations from the reference line (see Figs S1–S3), suggesting that all variables reasonably met the assumption of normality. To assess whether any outliers affected our results, we re-ran our LMMs with the outliers removed and found that the point estimates were not drastically affected (Tables S1 and S2), so we present the results from our full dataset. However, violations of the model assumptions would not have affected our analyses given our focus on fixed effects, which tend to be unbiased even if assumptions are violated (LeBeau et al., 2018). 'Individual' was treated as a random effect, and 'appendage type' (pectoral versus pelvic) or 'species' was treated as a fixed effect for intraspecific and interspecific comparisons, respectively.

Large sample sizes are typically required to produce accurate estimates of a random slopes model (reviewed in Harrison et al., 2018), so we assumed that the slopes were similar across the individuals within a species based on our smaller sample size. Assuming common slopes in a LMM can increase the potential for false positives and false negatives when calculating *P*-values for null hypothesis testing (reviewed in Harrison et al., 2018); however, the present study focused on effect sizes (i.e. the magnitude of the effects or variables) rather than the *P*-values, so these outcomes do not detract from our analyses. Given that one of the objectives of this study was to quantify the mean differences (i.e. point estimates) and range of variation (i.e. interval estimates) in GRF production and yank between and within salamanders, our emphasis on calculating effect sizes is appropriate (Cohen, 1990) because of the limited information that often results from traditional methods of null hypothesis testing (Cumming, 2014).

To calculate the point estimates (i.e. mean values) and interval estimates (i.e. standard errors) of the fixed effects, we used the emmeans::emmeans() function (https://CRAN.R-project.org/package=emmeans). The coefficient of determination (percentage of the variation explained by each model) was calculated as Nagakawa's marginal R^2 ($R^2_{\mathrm{LMM(m)}}$; variation due to the fixed effects only) and conditional R^2 ($R^2_{\mathrm{LMM(c)}}$; variation due to the fixed and random effects) using the performance::r2_nagakawa() function (Lüdecke et al., 2019). Dynamic changes in GRF and yank were plotted by pooling individual trials for a given species, but results from the LMMs are reported in the tables to account for repeated trials within individuals.

We then ran additional statistical analyses to determine whether our kinetic variables were influenced by stance duration. Stance duration was relatively similar between the two salamanders for the forelimbs (*P. waltl*: 0.545±0.027 s; *A. tigrinum*: 0.526±0.026 s) and hindlimbs (*P. waltl*: 0.607±0.036 s; *A. tigrinum*: 0.596±0.036 s) but was lower for *P. barbarus* pectoral fins (0.388±0.026 s), so we created additional LMMs with the interaction between species and stance duration as a fixed effect for the comparisons between pectoral appendages. To determine whether including stance as an interaction term improved our models for the pectoral appendages, we used likelihood ratio tests (LRTs) between the reduced model (LMM with species as a fixed effect and individual as a random effect) and the full model (LMM with a species×stance duration interaction term as a fixed effect and individual as a random effect) using the stats::anova() function in R. Stance duration did not improve the model for the net GRF (LRT: chi-squared: 7.979, d.f.=4, P=0.092) and the vertical component of the GRF (LRT: chi-squared: 2.417, d.f.=3, P=0.491). Including stance as an interaction with species did improve the model for the mediolateral component of the GRF (LRT: chi-squared=20.323, d.f.=4, P=0.0004), the anteroposterior component of the GRF (LRT: chi-squared=41.086, d.f.=4, P<0.0001), the mediolateral angle of the GRF (LRT: chi-squared=19.818, d.f.=4, P=0.0005) and the anteroposterior angle of the GRF (LRT: chi-squared=48.640, d.f.=4, P<0.0001). However additional analyses (see Table S3 and 'Comparison of stance durations' of the Supplementary Materials and Methods) indicated that stance duration had minimal effects on the point estimates from our LMMs and that these differences had no effect on the main patterns of our results. As such, we report the results from our reduced models to provide more straightforward interpretations of the statistical analyses.

RESULTS

Force production between the pectoral appendages of mudskippers and salamanders

The forelimbs of *P. waltl* exhibited kinetics that were distinct from (and sometimes intermediate between) those of the pectoral fins of *P. barbarus* fish and the forelimbs of *A. tigrinum* salamanders (Fig. 2). Force production during terrestrial locomotion generally approximated a bell-shaped curve that was skewed to the right in *P. barbarus* and *A. tigrinum*, but relatively broad and shallow in *P. waltl* for the net GRF and the vertical component of the GRF (Fig. 2A,B). The mediolateral component of the GRF was directed medially during stance for all three species, yet had a wider range of values in *P. barbarus* (Fig. 2C). For the anteroposterior component of the GRF, forelimb kinetics in *P. waltl* were more similar to those of terrestrial *A. tigrinum* salamanders than to semi-aquatic *P. barbarus* fish. The pectoral fin is the primary propulsor during crutching for *P. barbarus* and its GRF was oriented anteriorly for all of stance (indicating an acceleratory role), whereas the forelimbs of *A. tigrinum* and *P. waltl* showed primarily posteriorly directed GRFs (deceleratory role), with only one or two periods in which the GRFs became slightly anterior (Fig. 2D,F). The GRF was angled medially in the horizontal plane throughout stance for *P. barbarus* and *A. tigrinum*, and for almost all of stance for *P. waltl* except for a slight lateral orientation starting around 90% of stance (Fig. 2E). These findings illustrate how different aspects of force production by the forelimbs of *P. waltl* share similarities with those of semi-aquatic fins and terrestrial limbs, yet also show distinct differences (e.g. mediolateral GRFs).

GRF parameters at the peak net GRF also differed between the pectoral appendages for the three groups examined. The timing of the peak net GRF occurred at 60.4±2.86% of stance for *A. tigrinum*, 56.0±2.86% for *P. barbarus* and 46.9±2.93% for *P. waltl* (mean±s.e.m.; $R^2_{\mathrm{LMM(m)}}$=0.226, $R^2_{\mathrm{LMM(c)}}$=0.462). The magnitude of the peak net GRF was comparable between *P. barbarus* and *A. tigrinum* at approximately 44% and 46% of body weight, respectively, but was roughly 40% of body weight and had a wider range of values in *P. waltl* (Table 1, Fig. 3A). Similarly, the vertical component at the peak net GRF was comparable for *A. tigrinum* and *P. barbarus* yet lower and broader for *P. waltl* (Fig. 3B). The mediolateral component at the peak net GRF was similar between the two salamanders (Fig. 3C), with values for *P. barbarus* being 1.5–2 times more medial than those of the salamanders. The anteroposterior component was also more similar between the salamanders at the peak net GRF, with values being anterior (acceleratory) for *P. barbarus* but posterior (deceleratory) for both salamanders (Fig. 3D). The angle of the GRF was medial for all pectoral appendages at peak net GRF, but mean values for *P. waltl* were intermediate (−14 deg) between those of *P. barbarus* (−17 deg) and *A. tigrinum* (−9 deg) (Fig. 3E). These comparisons further demonstrate that kinetics at the time of peak net GRF for *P. waltl* share similarities with those of semi-aquatic fins and terrestrial limbs, with some features intermediate between the other two species.

Journal of Experimental Biology (2022) 225, jeb242795. doi:10.1242/jeb.242795

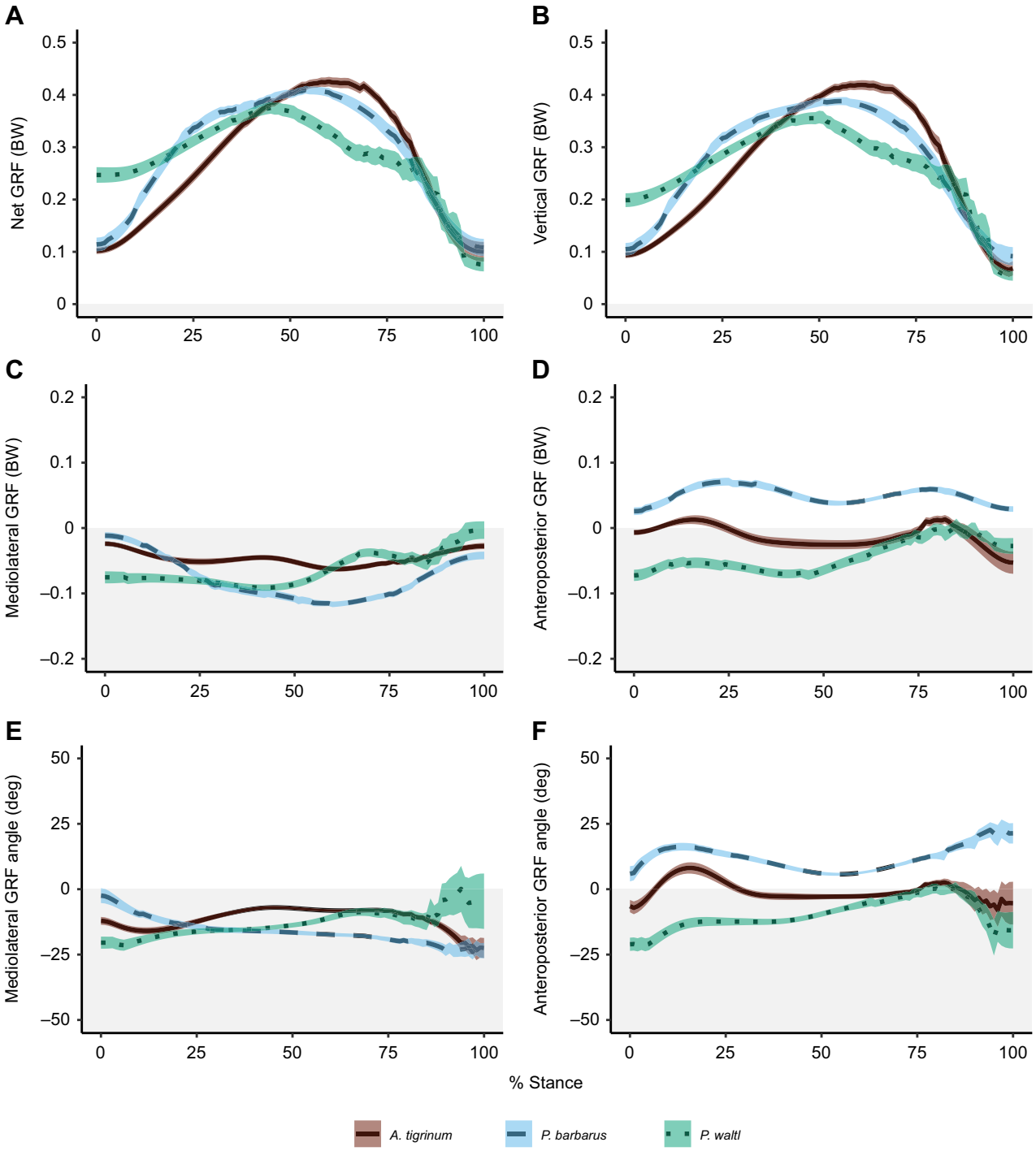

Fig. 2. Profiles of ground reaction force (GRF) production in the pectoral appendages during stance. (A) Net GRF, (B) vertical GRF, (C) mediolateral GRF, (D) anteroposterior GRF, (E) mediolateral GRF angle and (F) anteroposterior GRF angle. Individual trials were pooled within each species (*N*=50 trials for each) and profiles are plotted as the mean±s.e.m. for each percentage of stance. Mediolateral angles were set relative to vertical (0 deg), so negative values indicate a medial direction of the GRF. Anteroposterior angles were set relative to vertical (0 deg), so negative values represent a posterior direction of the GRF. Although the general shapes of the curves were comparable across the species for a given parameter, pectoral appendages for *P. waltl* tended to support lower magnitudes of body weight (BW), and have a more deceleratory role and intermediate mediolateral angle, compared with those of the semi-aquatic *P. barbarus* and the primarily terrestrial *A. tigrinum*.

Force production between salamander forelimbs and hindlimbs

Kinetic profiles were similar in shape between the hindlimbs of semi-aquatic and terrestrial salamanders (Fig. 4), but there were differences in the magnitudes of the curves. Semi-aquatic and terrestrial hindlimbs had a peak net GRF occurring around 30% of stance; however, the net GRF and the vertical component at peak GRF for *P. waltl* hindlimbs [0.349 and 0.314 body weight (BW), respectively] were more similar to those of *P. waltl* forelimbs (at about 30% of body weight) than to those of the hindlimbs of *A. tigrinum* (~50% of body weight) (Table 1, Fig. 5A,B). The GRFs were directed medially for all limbs (−9 to −17 deg) but were 1.5

Journal of Experimental Biology

Table 1. Comparison of locomotor variables between the appendages of mudskippers and salamanders at the peak net ground reaction force (GRF)

	Periophthalmus barbarus n=50		*Pleurodeles waltl n*=50		*Ambystoma tigrinum n*=50		Goodness-of-fit	
	FE±s.e.m.	CI	FE±s.e.m.	CI	FE±s.e.m.	CI	$R^2_{LMM(m)}$	$R^2_{LMM(c)}$
Pectoral appendages								
Net GRF (BW)	0.443±0.014	0.412, 0.473	0.404±0.015	0.372, 0.436	0.458±0.014	0.427, 0.488	0.090	0.183
Vertical GRF (BW)	0.417±0.012	0.392, 0.442	0.381±0.012	0.355, 0.407	0.447±0.012	0.422, 0.473	0.136	0.175
Mediolateral GRF (BW)	−0.129±0.012	−0.155, −0.102	−0.087±0.013	−0.114, −0.060	−0.067±0.012	−0.094, −0.041	0.256	0.497
Anteroposterior GRF (BW)	0.048±0.013	0.020, 0.076	−0.086±0.013	−0.115, −0.057	−0.029±0.013	−0.058, 0.0008	0.551	0.671
Mediolateral angle (deg)	−17.04±1.36	−20.0, −14.06	−13.62±1.40	−16.7, −10.56	−8.64±1.36	−11.6, −5.66	0.259	0.400
Anteroposterior angle (deg)	6.70±1.60	3.21, 10.20	−12.38±1.64	−15.95, −8.81	−3.32±1.60	−6.83, 0.16	0.598	0.692
Pelvic appendages								
Net GRF (BW)			0.362±0.021	0.315, 0.410	0.496±0.021	0.449, 0.543	0.506	0.712
Vertical GRF (BW)			0.332±0.024	0.276, 0.388	0.464±0.024	0.408, 0.520	0.452	0.728
Mediolateral GRF (BW)			−0.093±0.014	−0.125, −0.062	−0.072±0.014	−0.103, −0.040	0.043	0.317
Anteroposterior GRF (BW)			0.085±0.017	0.047. 0.124	0.133±0.017	0.094, 0.172	0.140	0.418
Mediolateral angle (deg)			−15.39±1.92	−19.80, −10.96	−9.22±2.192	−13.70, −4.79	0.154	0.383
Anteroposterior angle (deg)			14.9±2.72	8.59, 21.10	16.70±2.71	10.39, 22.90	0.009	0.342

Statistical analyses were based on the model: lmer(y ~ Species+(1|Individual), REML=True). Fixed effect (FE) values, s.e.m. and confidence intervals (CI) were estimated from the linear mixed effects model using the emmeans R package. $R^2_{LMM(m)}$ represents the variance explained by the fixed effects whereas $R^2_{LMM(c)}$ represents the variance explained by the combination of fixed and random effects; they were calculated using the performance::r2_nakagawa() function in R. BW, body weight.

and 2 times more medial in *P. waltl* than in *A. tigrinum* for the forelimbs and hindlimbs, respectively (Table 1, Fig. 5E). The forelimbs of both salamander species had a net decelerator role (Table 1), whereas the hindlimbs had a net acceleratory role (Table 1), with the hindlimbs of *A. tigrinum* showing a mean value ∼1.5 times higher than those of *P. waltl* at the time of peak net GRF (Fig. 5D). However, the angle of the GRF in the anteroposterior direction was comparable between salamander hindlimbs, inclined 16–17 deg anteriorly (Fig. 5F). These findings demonstrate that hindlimb kinetics are not necessarily equivalent between salamander species with differing degrees of terrestriality, and that locomotor biomechanics differ between the forelimbs and hindlimbs during terrestrial walking in both species.

Rate of change in GRF production

Average yank values for the pectoral appendages tended to be similar between the three species, but GRFs produced by the forelimbs of *P. waltl* generally reached their peak more slowly (as indicated by smaller absolute magnitudes of yank) and had a narrower range compared with those of the semi-aquatic fish and terrestrial salamanders (Table 2). The shapes of the curves for yank differed between *P. waltl* and the other two species. For *P. barbarus* and *A. tigrinum*, yank for the net GRF and vertical component of the GRF (Fig. 6A,B) approximated sine waves that started close to zero at the beginning of stance, increased to positive yank values before decreasing to an inflection point around 60% of stance, and then decreased to negative yank values before returning to the zero baseline. In contrast, the net GRF and vertical component of the GRF for *P. waltl* reached an inflection point at ∼50% of stance, and then approached zero again at ∼80% of stance, at a time when *A. tigrinum* and *P. barbarus* were both reaching their minimum yank values (i.e. peak in negative yank). The anteroposterior component was comparable between the two salamander forelimbs (∼0.006–0.008 BW for each percentage of stance), which increased faster than that for the pectoral fin of *P. barbarus* (0.004±0.001 BW for each percentage of stance). These findings demonstrate that rates of GRF production in the pectoral appendages of the semi-aquatic salamander, *P. waltl*, were generally comparable in magnitude but shifted at different times during stance and encompassed a narrower range of values than for the other two species.

Similarities between *A. tigrinum* and *P. waltl* were more evident in the shapes of the yank curves for the hindlimbs (Fig. 7). The curves for the net GRF (Fig. 7A) and the vertical component of the GRF (Fig. 7B) approximated sine waves that reached an inflection point at around 25% of stance. The peak for positive yank appears almost 2 times higher in *A. tigrinum* than in *P. waltl* (Fig. 7, Table 2), but the confidence intervals overlapped for the fixed effects. The minima for negative yank in the vertical component and net GRF were shallower in *P. waltl* than in *A. tigrinum*. As a result, rates of change in GRF production for the hindlimb were slower for the semi-aquatic *P. waltl* salamander compared with those in the terrestrial *A. tigrinum* salamander for the vertical component of the GRF and net GRF but profiles for yank in the mediolateral and anteroposterior directions were similar between the two taxa.

DISCUSSION

Comparisons of GRF patterns

Pleurodeles waltl is a semi-aquatic salamander that spends most of its life history underwater. Similar to terrestrial salamanders, the predominant acceleratory forces in this semi-aquatic salamander are produced by the hindlimb, signifying rear-wheel drive. The orientation of the GRF in the hindlimb was about 17 deg in the anterior direction for both salamanders, but more medial in *P. waltl* (−17 deg) than in *Ambystoma tigrinum* (−9 deg). Similarly, the orientation of the GRF for the pectoral appendages was more medial in the semi-aquatic *P. waltl* and *P. barbarus* than in the primarily terrestrial *A. tigrinum*; however, the anteroposterior GRF of both salamanders indicated a net deceleratory force compared with the acceleratory role in *P. barbarus* (Table 1). These differences in orientation may affect how loads are applied to the appendages, potentially resulting in the lower vertical component and net magnitude of the GRF in *P. waltl* forelimbs and hindlimbs.

Although the forelimbs of both salamanders had a net deceleratory role as evidenced by the negative value for the anteroposterior component of the GRF, this value was larger in magnitude throughout almost all of stance in *P. waltl*, whereas *A. tigrinum* exhibited two periods of slightly net positive values (Fig. 2, Table 1). Comparisons between the limbs of *P. waltl* demonstrate that the hindlimbs are the primary propulsors, whereas the forelimbs may be operating as ‘struts’ that act as pivot points about which the

Journal of Experimental Biology (2022) 225, jeb242795. doi:10.1242/jeb.242795

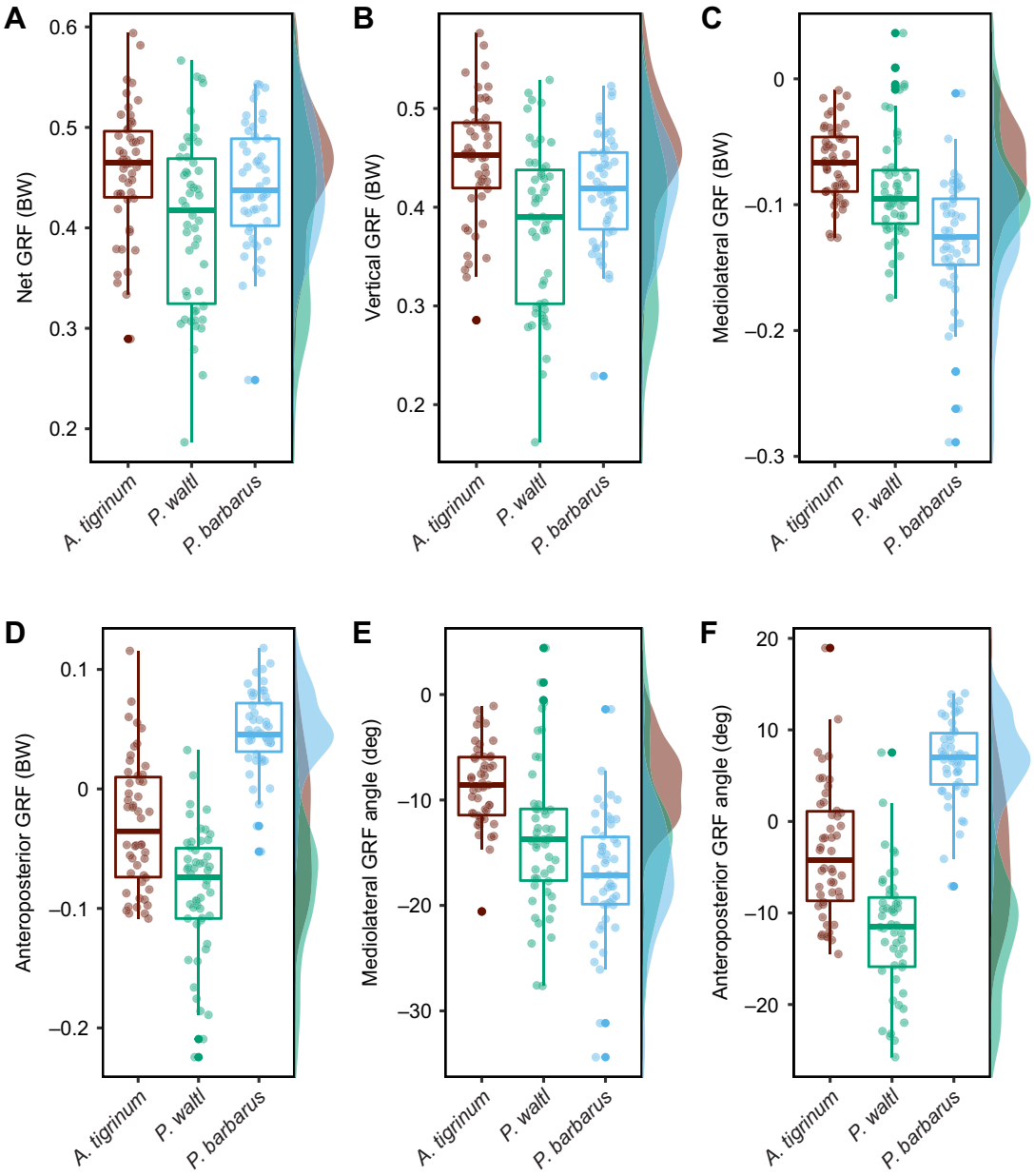

Fig. 3. Parameters at the peak net GRF compared across the pectoral appendages. (A) Net GRF, (B) vertical GRF, (C) mediolateral GRF, (D) anteroposterior GRF, (E) mediolateral GRF angle and (F) anteroposterior GRF angle. *Pleurodeles waltl* generally has lower magnitudes for the vertical component and net GRF, yet also had a greater variability compared with the semi-aquatic fish *P. barbarus* and the primarily terrestrial salamander *A. tigrinum* as illustrated by the box and whisker plots. Sample sizes for data from the pectoral appendages: *P. barbarus* n=50, *P. waltl* n=50 and *A. tigrinum* n=50.

body can rotate, based on observations that the extended limb angles produce a straightened limb and that the net role of the forelimbs is deceleratory (interpreted from the negative values of the anteroposterior component of the GRF). Semi-aquatic and terrestrial salamanders both exhibit functional disparities between their forelimbs and hindlimbs but the extent of these differences is more distinct in semi-aquatic salamanders, potentially suggesting greater functional decoupling of the locomotor roles (e.g. acceleratory versus deceleratory) in forelimbs and hindlimbs in more aquatic taxa.

Biomechanical differences between forelimbs and hindlimbs can be affected by limb proportions, kinematics and muscle anatomy, but these are unlikely to be the primary factors driving the patterns in our results. Differential limb function in running quadrupedal lizards was caused by interspecific differences in limb morphology, with a more medial orientation of the GRFs produced by the hindlimb in lizard species that had disproportionately longer hindlimbs than forelimbs (McElroy et al., 2014). In our study, patterns of GRF production differed between the forelimbs and hindlimbs within each salamander species, but the ratio between forelimb length and hindlimb length was ∼1 in *P. waltl* (Trochet et al., 2014) and the ratio between the diaphysis of the humerus to the femur was ∼1.19 and ∼1.03 in *A. tigrinum* and *P. waltl*, respectively (Molnar, 2021). Moreover, the muscular anatomy and kinematics of terrestrial walking were suggested to be relatively conserved within salamanders, but did exhibit some interspecific differences that could be due to the terrestriality of a given species, or other factors related to the physiological challenges that salamanders experience in their respective environments (Pierce et al., 2020). Differences in

Journal of Experimental Biology (2022) 225, jeb242795. doi:10.1242/jeb.242795

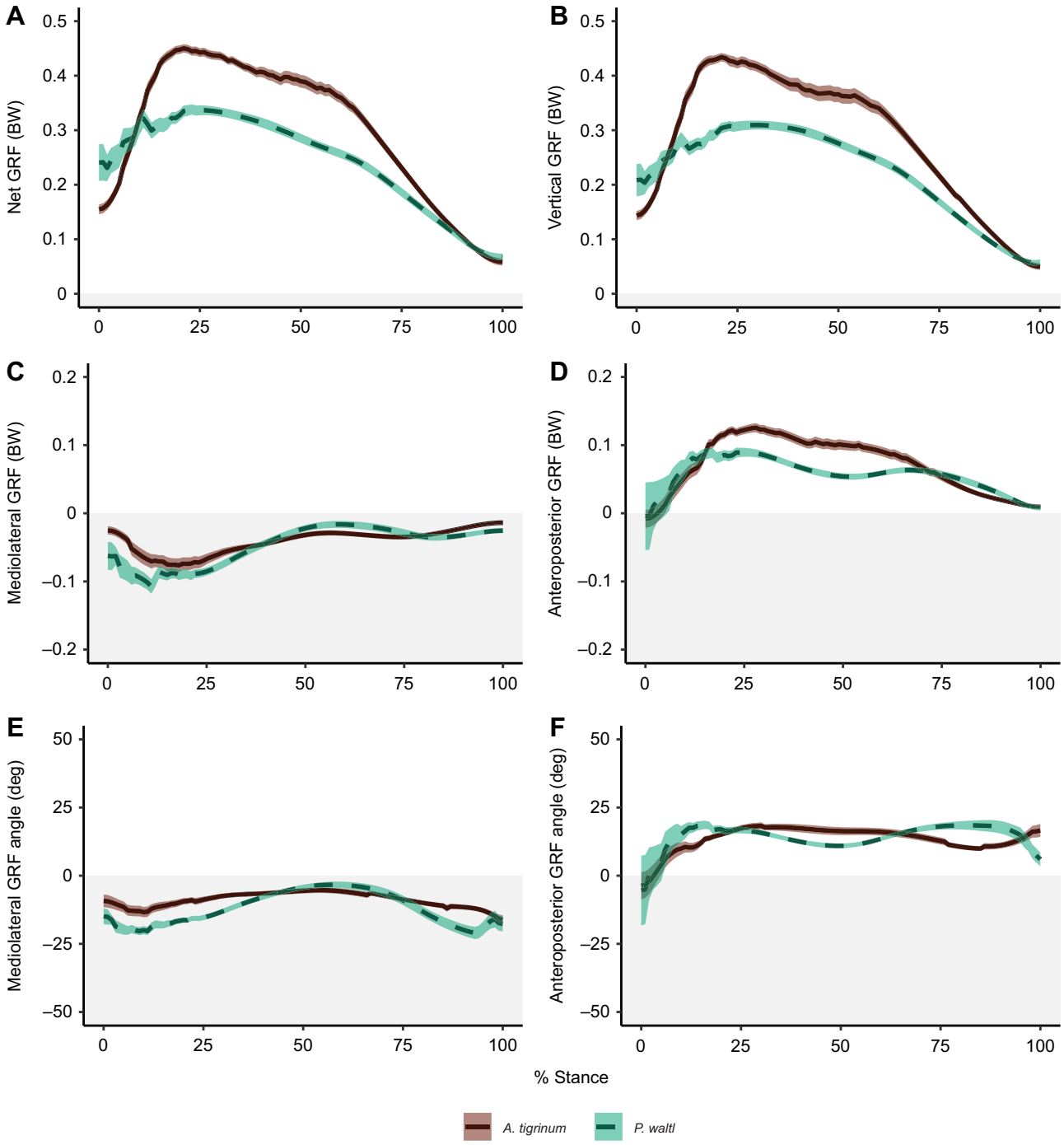

Fig. 4. Profiles of GRF production in the pelvic appendages during stance. (A) Net GRF, (B) vertical GRF, (C) mediolateral GRF, (D) anteroposterior GRF, (E) mediolateral GRF angle and (F) anteroposterior GRF angle. Individual trials were pooled within each species (*N*=49 trials for each) and profiles are plotted as the mean±s.e.m. for each percentage of stance. Mediolateral angles were set relative to vertical (0 deg), so negative values indicate a medial direction of the GRF. Anteroposterior angles were set relative to vertical (0 deg), so negative values represent a posterior direction of the GRF. Although the general shapes of the curves were comparable across the species for a given parameter, *P. waltl* hindlimbs tended to support lower magnitudes of body weight (BW) and had less of an acceleratory role compared with those of the primarily terrestrial salamander *A. tigrinum*.

ecological factors between our salamander species (e.g. habitual environments) could, thus, play a larger role in shaping GRF patterns than differences in anatomy or kinematics.

The functional differences between (i) pectoral and pelvic appendages and (ii) aquatic and terrestrial species could relate to the different demands imposed by the primary environments in which the appendages of these taxa function. For example, point estimates for the medial orientation of the peak GRF in semi-aquatic *P. waltl* limbs (−14 to −16 deg, forelimb–hindlimb) fall between those of *P. barbarus* pectoral fins (−17 deg) and most previously evaluated tetrapod limbs (≤−11 deg), including primarily terrestrial *A. tigrinum* salamanders (Fig. 8, Tables 1 and 2). A shift to a GRF directed less medially could reduce joint moments and, thus, the stresses experienced by the appendicular bones during terrestrial locomotion (Kawano and Blob, 2013). However, the greater medial orientation of the GRF in semi-aquatic *P. waltl* likely relates to the

Journal of Experimental Biology (2022) 225, jeb242795. doi:10.1242/jeb.242795

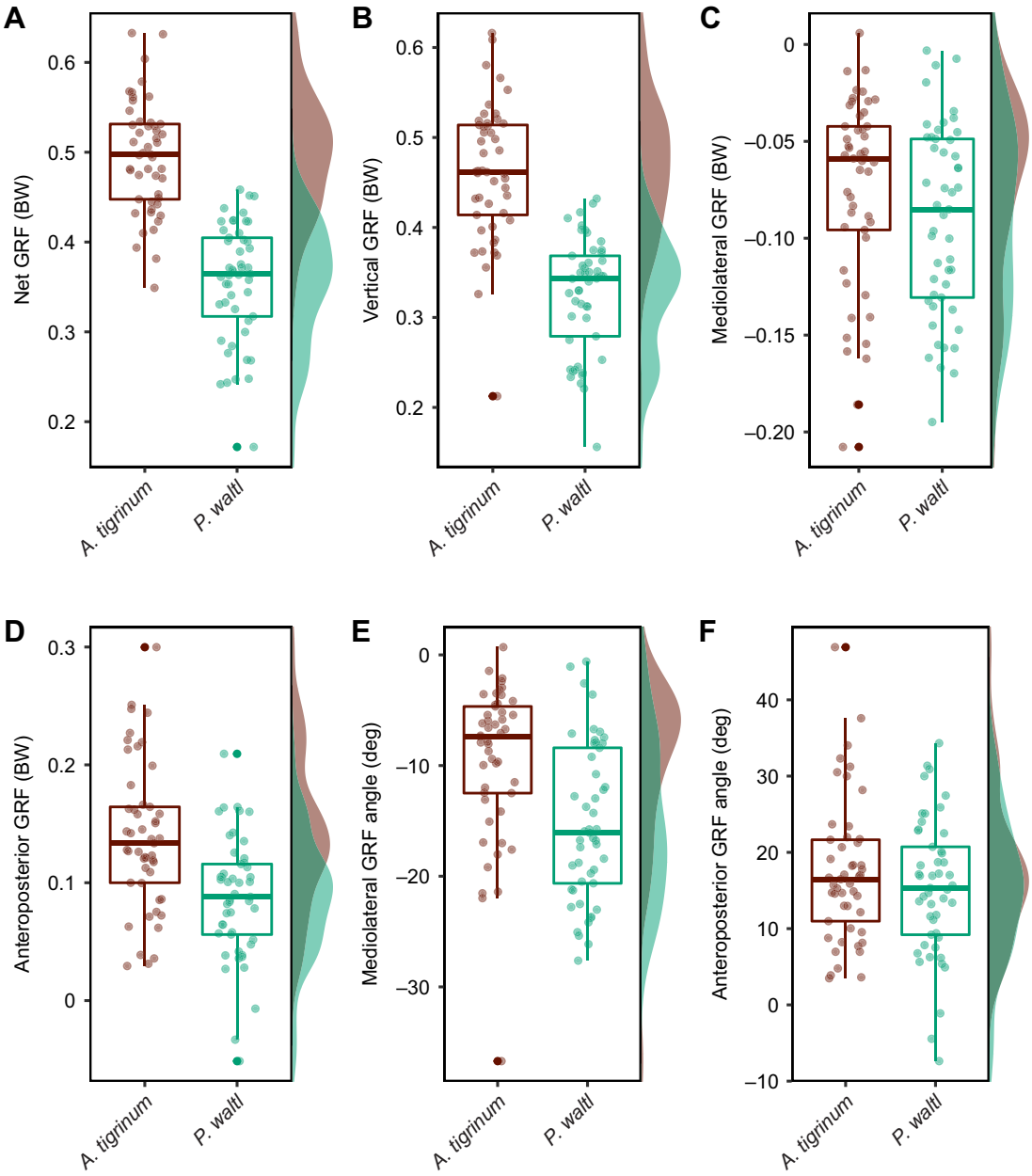

Fig. 5. Parameters at the peak net GRF compared across the pelvic appendages. (A) Net GRF, (B) vertical GRF, (C) mediolateral GRF, (D) anteroposterior GRF, (E) mediolateral GRF angle and (F) anteroposterior GRF angle. *Pleurodeles waltl* hindlimbs generally had lower magnitudes for the vertical component and net GRF, yet the angle of GRF orientation could become almost 2 times more medial than for the primarily terrestrial salamander *A. tigrinum*, as illustrated by the box and whisker plots. Sample sizes for the pelvic appendages: *P. waltl* *n*=49 and *A. tigrinum* *n*=49.

greater lateral spread of their distal limb segments compared with those of terrestrial salamanders, so that the feet are placed lateral to the elbow or knee joint during stance (Fig. 1B), rather than directly below these joints (as in terrestrial salamanders: Fig. 1C). A recent comparison of terrestrial locomotion in salamanders found that the maximum extensions of the wrist (160 deg), ankle (159 deg) and knee (155 deg) were higher in *P. waltl* than in *A. tigrinum* (150, 150 and 145 deg, respectively), and that the maximum abduction of the upper arm was larger in *P. waltl* (128 deg) than in *A. tigrinum* (110 deg) (Pierce et al., 2020). These kinematic differences could collectively contribute towards placing the distal elements of the limb more laterally in *P. waltl*. In addition, aquatic salamanders generally have thicker and longer articular cartilage on the long bones of their limbs (despite the forelimbs and hindlimbs being relatively subequal within taxa) and the thickness of the articular cartilage as a percentage of bone length was almost 2 times greater in *P. waltl* (52.3–43.7%, humerus–femur) than in *A. tigrinum* (24.1–24.8%, humerus–femur) (Molnar, 2021). Increasing the amount of cartilage on articular surfaces increases muscle length by moving the insertion point more distally, thereby increasing muscle leverage for limb extension (Molnar, 2021). *Taricha torosa*, another semi-aquatic salamander, had greater lateral spread of the limbs when walking in water than on land, which was caused by more extended angles about the limb joints (Ashley-Ross and Bechtel, 2004). Specifically, *T. torosa* had greater extension of the elbow and greater excursion of the elbow than *A. tigrinum* and *P. waltl*, while having comparable maximum extension of the knee and maximum abduction of the thigh (Pierce et al., 2020). Thus,

Journal of Experimental Biology (2022) 225, jeb242795. doi:10.1242/jeb.242795

Table 2. Range of average yank values compared between appendages and species

	Vertical		Mediolateral		Anteroposterior		Net	
	FE±s.e.m.	CI	FE±s.e.m.	CI	FE±s.e.m.	CI	FE±s.e.m.	CI
Pectoral – maximum								
P. barbarus	0.010±0.001	0.008, 0.012	0.004±0.001	0.003, 0.006	0.004±0.001	0.002, 0.005	0.011±0.001	0.008, 0.013
P. waltl	0.009±0.001	0.007, 0.011	0.006±0.001	0.004, 0.008	0.008±0.001	0.007, 0.010	0.009±0.001	0.007, 0.012
A. tigrinum	0.012±0.001	0.010, 0.014	0.004±0.001	0.002, 0.005	0.006±0.001	0.004, 0.008	0.012±0.001	0.010, 0.014
Pectoral – minimum								
P. barbarus	−0.012±0.001	−0.014, −0.010	−0.005±0.001	−0.006, −0.003	−0.004±0.001	−0.005, −0.003	−0.013±0.001	−0.015, −0.011
P. waltl	−0.009±0.001	−0.011, −0.007	−0.006±0.001	−0.008, −0.005	−0.005±0.001	−0.006, −0.003	−0.010±0.001	−0.012, −0.007
A. tigrinum	−0.013±0.001	−0.016, −0.011	−0.004±0.001	−0.006, −0.003	−0.007±0.001	−0.008, −0.005	−0.014±0.001	−0.016, −0.011
Pelvic – maximum								
P. waltl	0.005±0.001	0.002, 0.008	0.006±0.001	0.005, 0.008	0.006±0.001	0.004, 0.008	0.006±0.001	0.003, 0.009
A. tigrinum	0.010±0.001	0.007, 0.013	0.006±0.001	0.005, 0.008	0.009±0.001	0.007, 0.011	0.010±0.001	0.007, 0.014
Pelvic – minimum								
P. waltl	−0.009±0.001	−0.011, −0.007	−0.004±0.0004	−0.005, −0.003	−0.006±0.001	−0.007, −0.005	−0.009±0.001	−0.012, −0.007
A. tigrinum	−0.014±0.001	−0.016, −0.012	−0.004±0.0004	−0.005, −0.003	−0.007±0.001	−0.008, −0.006	−0.015±0.001	−0.017, −0.012

Sample sizes for the pectoral yank linear mixed models (LMM): *P. barbarus* n=50, *P. waltl* n=50 and *A. tigrinum* n=50. Sample sizes for the pelvic yank LMM: *P. waltl* n=49 and *A. tigrinum* n=49. FE, estimates of the coefficients for the fixed effects based on estimated marginal means with the emmeans::emmeans() function. Statistical analyses were based on the model: lme4::lmer(y ~ species+(1 | individual), REML=True). The confidence interval (CI) is listed as the lower and upper bounds, respectively, that were reported from the LMMs.

certain aspects related to differences in the extensions in the proximal limb joints and abduction of the proximal limb elements (e.g. Pierce et al., 2020), articular cartilage (e.g. Molnar, 2021) and locomotor forces (this study) may collectively provide a stronger foundation for distinguishing semi-aquatic versus terrestrial salamanders. Given that this more pronounced lateral position of the distal limb segment is also found in the mudskipper fish, a more medial orientation of the GRF also might be found in other semi-aquatic taxa.

The observation that *P. waltl* generally has more extended joint angles than terrestrial salamanders on land may mean that some salamanders exhibit stereotypy (*sensu* Wainwright et al., 2008) in their locomotor biomechanics. The wider spread of the limbs that would result from such lateral foot placement might convey additional stability against currents or other flows in aquatic habitats (Martinez et al., 1998) by reducing pitching and rolling (Chen et al., 2006). However, when on land, species that tend to be more aquatic may not be able to adjust to the more upright orientations of distal limb segments that are seen in terrestrial taxa (Kawano and Blob, 2013). Producing more acute angles about the more proximal joints could facilitate elevating the body off the ground, and shift the bone loading regime to reduce bending and increase compression (Ashley-Ross and Bechtel, 2004; Kawano and Blob, 2013), but the latter has yet to be confirmed empirically. Lateral spread of the distal appendage may also contribute to the high medial orientation of the GRF in mudskippers (Figs 1 and 2), and could prevent rolling of the body axis during terrestrial crutching, given the lack of extended posterior appendages in this taxon. Thus, shifts to less sprawling limb posture by flexing the distal limb segments closer to the body could have major biomechanical consequences that could facilitate terrestrial locomotion.

Comparisons of yank and its relevance to bone loading

Similarities in the overall shapes of GRF and yank profiles produced by individual hindlimbs suggest that rates of GRF production are consistent in the timing of their changes across hindlimbs of semi-aquatic and terrestrial salamander species, but the different peaks observed in these curves indicate that the maxima differ between them. The similarities in force production between semi-aquatic and terrestrial hindlimbs could indicate that the use of the hindlimbs as a primary propulsor imposes strong constraints on kinetics for acceleration, but that other aspects, such as maneuverability and body support, can be altered by changing the GRFs and yank. For example, the smaller absolute value in the vertical component of the GRF and net GRF for the hindlimbs in *P. waltl*, compared with *A. tigrinum*, suggest that there may be steadier (i.e. less variable) loads in the former. Loading the appendages in more predictable ways can have numerous advantages (Granatosky et al., 2020). For instance, higher safety factors (margins of protection against failure) may be found in structures that experience more variable loading (Alexander, 1997; Lowell, 1985). Consequently, steadier loading could reduce the safety factors needed in the limb bones and, therefore, reduce the energetic costs to produce the higher safety factors. If load magnitudes were elevated as a result of the highly sprawled posture of *P. waltl* (Fig. 8), then it would be advantageous to have less variation in bone loading to reduce the safety factors needed. The limb bones of *A. tigrinum* have been found to possess generally high safety factors against failure (Blob et al., 2014; Kawano et al., 2016; Sheffield and Blob, 2011) and studies are ongoing to determine whether a similar pattern is found in semi-aquatic salamanders.

The rate of load application can also affect the load magnitudes experienced by bones. Strain magnitude is positively correlated with strain rate for both cyclic and discrete loading regimes in vertebrates (Aiello et al., 2015), so smaller yank values in *P. waltl* may be associated with slower strain rates and lower peak strain magnitudes in their limb bones. Lower peak strains would keep bones further from failure, whereas slower strain rates could affect bone mass (Rubin and Lanyon, 1982). Thus, peak strains could have a direct impact on the safety factors of the limb bones, and strain rates could affect the remodeling of bones in response to different loading patterns. Strain rate has been found to be a main factor driving bone remodeling and was positively correlated with higher Young's modulus values (Aiello et al., 2015), which would confer greater stiffness and greater resistance to bending in bones. Such properties would be advantageous for terrestrial taxa that must habitually withstand the downward effects of gravity on land. Semi-aquatic taxa that spend most of their time underwater might not need higher stiffness in their limb bones while their bodies are primarily being supported by buoyancy; however, such traits could be

Journal of Experimental Biology (2022) 225, jeb242795. doi:10.1242/jeb.242795

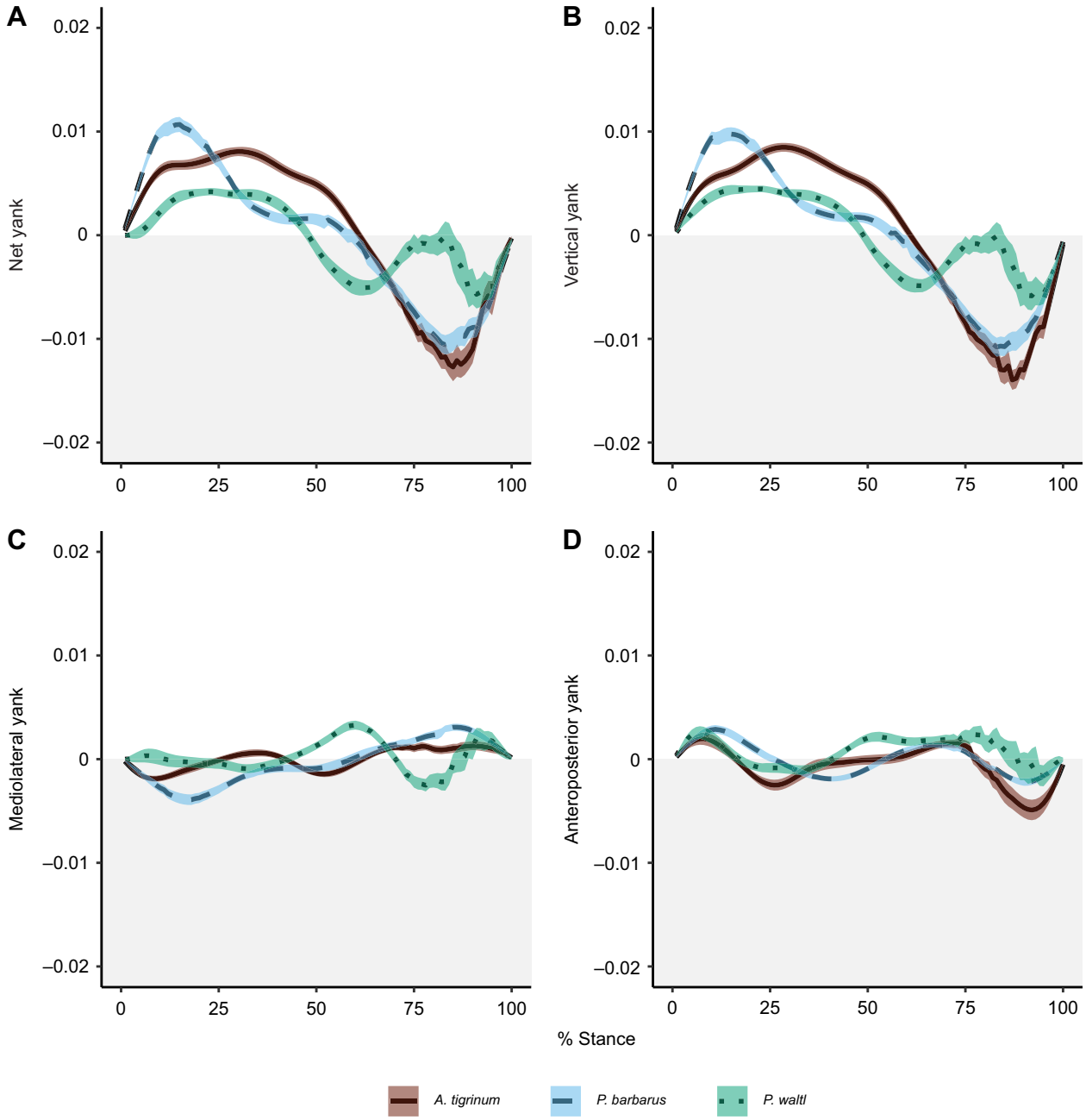

Fig. 6. Profiles of the rate of GRF production (yank) in the pectoral appendages during stance. (A) Net yank, (B) vertical yank, (C) mediolateral yank and (D) anteroposterior yank. Individual trials were pooled within each species (*N*=50 trials for each) and profiles are plotted as the mean±s.e.m. for each percentage of stance. Mediolateral components were set relative to vertical (0 deg), so negative values indicate a medial direction of the GRF. Anteroposterior components were set relative to vertical (0 deg), so negative values represent a posterior direction of the GRF. Yank values for *P. waltl* tended to span a narrower range of values and did not generally follow the same shape dynamics as those of the semi-aquatic fish *P. barbarus* and the primarily terrestrial salamander *A. tigrinum*, which tended to yield comparable data.

beneficial during the terrestrial eft phase of many newt species (including *P. waltl*). Preliminary analyses on the cross-sectional geometry of the limb bones in 93 salamander species indicate that the second moment of area at the mid-shaft is greater in terrestrial salamanders, suggesting a higher resistance to bending, compared with aquatic salamanders (Huie et al., in press). Changes in the mechanical properties and loading regimes of limb bones across ontogenetic stages within salamanders and between species with different life histories (e.g. direct versus indirect developers) are the subject of subsequent studies by our labs and would provide further insight into the factors that shape limb function.

Functional diversity in locomotor biomechanics in the context of water–land transitions

Comparative studies on the locomotor biomechanics of salamanders living in different environments lend valuable information about the realm of locomotor capabilities that are possible within a general tetrapod Bauplan and point towards new avenues for examining the functional differences between and within limbs in the context of water–land transitions (Pierce et al., 2013; Standen et al., 2014). Broadening empirical analyses of extant taxa to include variation in ecology and habitat use is particularly crucial to identify which characteristics may confer greater terrestrial

Journal of Experimental Biology (2022) 225, jeb242795. doi:10.1242/jeb.242795

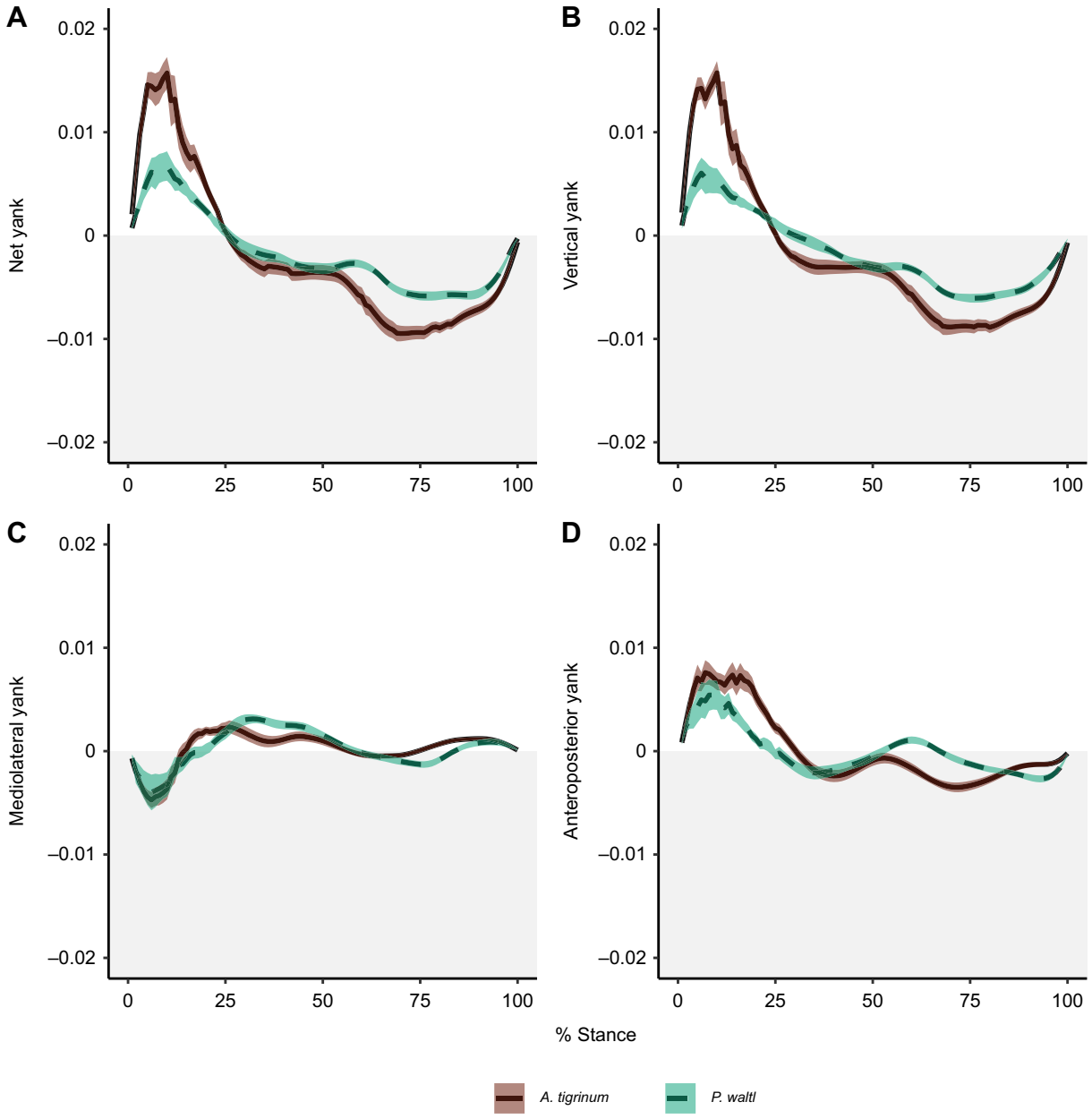

Fig. 7. Profiles of the rate of GRF production (yank) in the pelvic appendages during stance. (A) Net yank, (B) vertical yank, (C) mediolateral yank and (D) anteroposterior yank. Individual trials were pooled within each species (*N*=49 trials for each) and profiles are plotted as the mean±s.e.m. for each percentage of stance. Mediolateral components were set relative to vertical (0 deg), so negative values indicate a medial direction of the GRF. Anteroposterior components were set relative to vertical (0 deg), so negative values represent a posterior direction of the GRF. Yank values for *P. waltl* hindlimbs tended to span a narrower range of values for the vertical component and net GRF, but were otherwise relatively comparable to those from the primarily terrestrial salamander *A. tigrinum*.

capabilities. Although limb kinematics and neuromuscular control during terrestrial locomotion appear to be relatively conserved across extant salamanders (Pierce et al., 2020), other aspects have been found to vary between aquatic and terrestrial salamanders. Terrestrial salamanders tend to have greater resistance to bending (Huie et al., 2022), shorter and thinner articular cartilage (Molnar, 2021), and decreased compactness via larger medullary cavities (Canoville and Laurin, 2009; Laurin et al., 2011) in their limb bones compared with aquatic salamanders. Amphibious salamanders are a particular challenge given that they sometimes cannot be differentiated from their terrestrial counterparts (Laurin et al., 2011) or have features that overlap with those of both aquatic and terrestrial salamanders (Molnar, 2021). Our work adds to this area of research by demonstrating how differences in the locomotor functions of forelimbs versus hindlimbs within a salamander can be less pronounced in a primarily terrestrial taxon, prompting future studies to examine whether the locomotor modules within salamanders exhibit different levels of integration in aquatic versus terrestrial species and environments.

Taxa with intermediate morphologies and locomotor biomechanics may be particularly relevant for improving understanding of stem tetrapods. Morphological comparisons across the humeri of 40 tetrapodomorphs spanning the water–land transition demonstrated that stem tetrapods had intermediate morphologies that placed them in a valley between two adaptive

Journal of Experimental Biology (2022) 225, jeb242795. doi:10.1242/jeb.242795

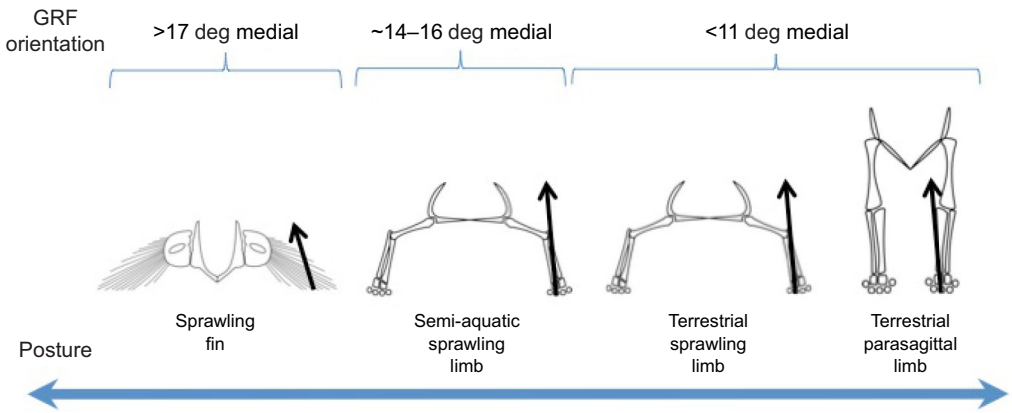

Fig. 8. Orientation of the GRF across vertebrates. Data on GRF production in semi-aquatic *P. waltl* salamanders contribute towards a broader perspective on the evolution of the locomotor biomechanics across the fish–tetrapod transition. The orientation of the GRF (represented as a black arrow) in the medial direction was historically thought to be evolutionarily conserved across tetrapods, despite variation in limb postures. It was unclear whether the same pattern was found in fishes, but our previous work found that GRFs produced by pectoral fins in mudskipper fishes were more medial, likely resulting from their more sprawled posture compared with that of tetrapods. GRF data from *P. waltl* in this study demonstrate that the more medial orientation of GRFs is not exclusive to fishes, suggesting that ecology may have an important role in shaping the kinetics during terrestrial locomotion.

peaks (one for aquatic fishes and a second for terrestrial crown tetrapods) (Dickson et al., 2021). This was a likely transitional state before natural selection was strong enough to favor the movement of stem tetrapods to the adaptive peak representing the terrestrial characteristics now associated with crown tetrapods (Dickson et al., 2021). Moreover, *Pederpes* is an early tetrapod from the Early Carboniferous (348–344 million years ago) and had some terrestrial adaptations (e.g. forward-pointing foot) (Clack, 2009) but recent analyses indicated that there were also other traits that were indistinguishable from the Devonian early tetrapod (~365 million years ago) *Acanthostega*, which was likely fully aquatic (Molnar et al., 2021), suggesting that early tetrapods in the early Carboniferous possessed a mosaic of tetrapod-like and fish-like traits that may have limited extended excursions on land. In addition, *Greererpeton burkemorani* is another early tetrapod from the Early Carboniferous (about 335–331 million years ago) that was presumed to be benthic and primarily aquatic (Godfrey, 1989). Our preliminary analyses on the locomotor capabilities of *G. burkemorani* indicated that estimated peak stresses in the femur decreased when modeling it with peak GRF magnitudes that more closely resembled those of the semi-aquatic *P. waltl* and as the angle between the GRF and the femur resembled more sprawling limb postures (Kawano and Blob, 2020). These studies highlight how incorporating a range of terrestrial capabilities can help broaden perspectives on the biology of stem tetrapods that likely still possessed a mosaic of tetrapod-like and fish-like features that are more indicative of a semi-aquatic taxon, rather than a fully aquatic or fully terrestrial taxon.

Conclusion

Our results provide novel insights into the functional changes associated with tetrapods becoming terrestrial, with broader implications for whether functional capabilities could be closely associated with major structural changes (e.g. transition from fin to limb) or could occur through gradual changes that included intermediate stages where taxa possess a mix of fish-like and tetrapod-like features. The kinetics of terrestrial walking in semi-aquatic *P. waltl* salamanders differed between the limbs, with the hindlimbs sharing numerous similarities with the hindlimbs of primarily terrestrial salamanders but the forelimbs exhibiting kinetics that were distinct from those of the pectoral appendages of both semi-aquatic fish and primarily terrestrial salamanders. Differences in limb kinetics between *P. waltl* and *A. tigrinum* could relate to the primary environments they inhabit as adults (i.e. aquatic and terrestrial, respectively), which complements published work demonstrating that limb morphology relates to a salamander's degree of terrestriality. Some kinetic patterns in *P. waltl* that were intermediate between those of semi-aquatic *P. barbarus* fins and terrestrial *A. tigrinum* limbs (e.g. mediolateral orientation of the GRF), which could be related to *P. waltl* possessing other traits (e.g. extended joint angles) that are intermediate between those of fishes and terrestrial salamanders. These data provide additional context to account for differential limb function in models of musculoskeletal function, including those that use salamanders as a blueprint for estimating the locomotor function of early tetrapods.

Acknowledgements

We thank Zach Marion, Jim Fordyce and Yu Xia for helpful discussions on statistical analyses that were considered for this study. We are also grateful to Margaret Ptacek, Miriam Ashley-Ross and the anonymous reviewers for feedback on earlier drafts of the manuscript. An earlier draft of the manuscript was submitted by S.M.K. in partial fulfilment of a doctoral dissertation at Clemson University.

Competing interests

The authors declare no competing or financial interests.

Author contributions

Conceptualization: S.M.K., R.W.B.; Methodology: S.M.K., R.W.B.; Software: S.M.K.; Validation: S.M.K.; Formal analysis: S.M.K.; Investigation: S.M.K.; Resources: R.W.B.; Data curation: S.M.K.; Writing - original draft: S.M.K., R.W.B.; Writing - review & editing: S.M.K., R.W.B.; Visualization: S.M.K.; Supervision: R.W.B.; Funding acquisition: S.M.K., R.W.B.

Funding

Funding to conduct this work was provided by the American Society for Ichthyologists and Herpetologists Gaige and Raney Awards, Sigma Xi Grants-in-Aid of Research, Society for Vertebrate Paleontology Estes Memorial Grant, and Clemson University Stackhouse Fellowship to S.M.K., and through the National Science Foundation (IOS 0517240 and IOS 0817794) to R.W.B.

Data availability

All R codes are available from GitHub (https://github.com/MorphoFun/kraken). The specific scripts for this paper are in the 'compareGRFs' folder; the raw files for the original force data are located in the 'force_rawFiles' folder; and the R script to calculate the GRF data and run the statistical analyses is called 'GRFAnalysis.R'.

References

Ahlberg, P. E. (2018). Follow the footprints and mind the gaps: a new look at the origin of tetrapods. *Earth Environ. Sci. Trans. R. Soc. Edinb* **109**, 115-137. doi:10.1017/S1755691018000695

Aiello, B. R., Iriarte-Diaz, J., Blob, R. W., Butcher, M. T., Carrano, M. T., Espinoza, N. R., Main, R. P. and Ross, C. F. (2015). Bone strain magnitude is correlated with bone strain rate in tetrapods: implications for models of mechanotransduction. *Proc. R. Soc. B Biol. Sci.* **282**, 20150321. doi:10.1098/rspb.2015.0321

Alexander, R. M. (1997). A theory of mixed chains applied to safety factors in biological systems. *J. Theor. Biol.* **184**, 247-252. doi:10.1006/jtbi.1996.0270

Ashley-Ross, M. A. (1994). Hindlimb kinematics during terrestrial locomotion in the salamander (*Dicamptodon tenebrosus*). *J. Exp. Biol.* **193**, 285-305. doi:10.1242/jeb.193.1.285

Ashley-Ross, M. A. and Barker, J. U. (2002). The effect of fiber-type heterogeneity on optimized work and power output of hindlimb muscles of the salamander Ambystoma tigrinum. *J. Comp. Physiol. A* **188**, 611-620. doi:10.1007/s00359-002-0336-4

Ashley-Ross, M. A. and Bechtel, B. F. (2004). Kinematics of the transition between aquatic and terrestrial locomotion in the newt *Taricha torosa*. *J. Exp. Biol.* **207**, 461-474. doi:10.1242/jeb.00769

Ashley-Ross, M. A., Lundin, R. and Johnson, K. L. (2009). Kinematics of level terrestrial and underwater walking in the California newt, *Taricha torosa*. *J. Exp. Zool.* **311A**, 240-257. doi:10.1002/jez.522

Ashley-Ross, M. A., Hsieh, S. T., Gibb, A. C. and Blob, R. W. (2013). Vertebrate land invasions – past, present, and future: An introduction to the symposium. *Integr. Comp. Biol.* **53**, 192-196. doi:10.1093/icb/ict048

Azizi, E. and Horton, J. M. (2004). Patterns of axial and appendicular movements during aquatic walking in the salamander *Siren lacertina*. *Zoology* **107**, 111-120. doi:10.1016/j.zool.2004.03.002

Bates, D., Maechler, M., Bolker, B. and Walker, S. (2015). Fitting linear mixed-effects models using lme4. *J. Stat. Softw.* **67**, 1-48. doi:10.18637/jss.v067.i01

Bennett, A. F., Garland, T. and Else, P. L. (1989). Individual correlation of morphology, muscle mechanics, and locomotion in a salamander. *Am. J. Physiol.* **256**, 1200-1208. doi:10.1152/ajpregu.1989.256.6.R1200

Blob, R. W. (2001). Evolution of hindlimb posture in nonmammalian therapsids: biomechanical tests of paleontological hypotheses. *Paleobiology* **27**, 14-38. doi:10.1666/0094-8373(2001)027<0014:EOHPIN>2.0.CO;2

Blob, R. W., Espinoza, N. R., Butcher, M. T., Lee, A. H., D'Amico, A. R., Baig, F. and Sheffield, K. M. (2014). Diversity of limb-bone safety factors for locomotion in terrestrial vertebrates: evolution and mixed chains. *Integr. Comp. Biol.* **54**, 1058-1071. doi:10.1093/icb/icu032

Boisvert, C. A. (2005). The pelvic fin and girdle of *Panderichthys* and the origin of tetrapod locomotion. *Nature* **438**, 1145-1147. doi:10.1038/nature04119

Brand, L. R. (1996). Variations in salamander trackways resulting from substrate differences. *J. Paleontol.* **70**, 1004-1010. doi:10.1017/S0022336000038701

Canoville, A. and Laurin, M. (2009). Microanatomical diversity of the humerus and lifestyle in lissamphibians. *Acta Zool.* **90**, 110-122. doi:10.1111/j.1463-6395.2008.00328.x

Chen, J. J., Peattie, A. M., Autumn, K. and Full, R. J. (2006). Differential leg function in a sprawled-posture quadrupedal trotter. *J. Exp. Biol.* **209**, 249-259. doi:10.1242/jeb.01979

Clack, J. A. (2009). The fin to limb transition: new data, interpretations, and hypotheses from paleontology and developmental biology. *Annu. Rev. Earth Planet. Sci.* **37**, 163-179. doi:10.1146/annurev.earth.36.031207.124146

Cohen, J. (1990). Things I have learned (so far). *Am. Psychol.* **45**, 1304-1312. doi:10.1037/0003-066X.45.12.1304

Cumming, G. (2014). The new statistics: why and how. *Psychol. Sci.* **25**, 7-29. doi:10.1177/0956797613504966

Deban, S. M. and Schilling, N. (2009). Activity of trunk muscles during aquatic and terrestrial locomotion in *Ambystoma maculatum*. *J. Exp. Biol.* **212**, 2949-2959. doi:10.1242/jeb.032961

Delvolvé, I., Bem, T. and Cabelguen, J. M. (1997). Epaxial and limb muscle activity during swimming and terrestrial stepping in the adult newt, *Pleurodeles waltl*. *J. Neurophysiol.* **78**, 638-650. doi:10.1152/jn.1997.78.2.638

Dickson, B. V., Clack, J. A., Smithson, T. R. and Pierce, S. E. (2021). Functional adaptive landscapes predict terrestrial capacity at the origin of limbs. *Nature* **589**, 242-245. doi:10.1038/s41586-020-2974-5

Fabre, A.-C., Bardua, C., Bon, M., Clavel, J., Felice, R. N., Streicher, J. W., Bonnel, J., Stanley, E. L., Blackburn, D. C. and Goswami, A. (2020). Metamorphosis shapes cranial diversity and rate of evolution in salamanders. *Nat. Ecol. Evol.* **4**, 1129-1140. doi:10.1038/s41559-020-1225-3

Frolich, L. M. and Biewener, A. A. (1992). Kinematic and electromyographic analysis of the functional role of the body axis during terrestrial and aquatic locomotion in the salamander *Ambystoma tigrinum*. *J. Exp. Biol.* **162**, 107-130. doi:10.1242/jeb.162.1.107

Gao, K. and Shubin, N. H. (2001). Late Jurassic salamanders from northern China. *Nature* **410**, 574-577. doi:10.1038/35069051

Godfrey, S. (1989). The postcranial skeletal anatomy of the carboniferous tetrapod *Greererpeton burkemorani* Romer, 1969. *Philos. Trans. R. Soc. Lond. B Biol. Sci.* **323**, 75-133. doi:10.1098/rstb.1989.0002

Granatosky, M. C., McElroy, E. J., Lemelin, P., Reilly, S. M., Nyakatura, J. A., Andrada, E., Kilbourne, B. M., Allen, V. R., Butcher, M. T., Blob, R. W. et al. (2020). Variation in limb loading magnitude and timing in tetrapods. *J. Exp. Biol.* **223**, jeb201525. doi:10.1242/jeb.201525

Harrison, X. A., Donaldson, L., Correa-Cano, M. E., Evans, J., Fisher, D. N., Goodwin, C. E. D., Robinson, B. S., Hodgson, D. J. and Inger, R. (2018). A brief introduction to mixed effects modelling and multi-model inference in ecology. *PeerJ* **6**, e4794. doi:10.7717/peerj.4794

Hohn-Schulte, B., Preuschoft, H., Witzel, U., Distler-Hoffmann, C. (2013). Biomechanics and functional preconditions for terrestrial lifestyle in basal tetrapods, with special consideration of *Tiktaalik roseae*. *Hist. Biol.* **25**, 167-181. doi:10.1080/08912963.2012.755677

Huie, J., Pyron, R. A. and Kawano, S. M. (in press). The effects of habitat and development on the evolution of salamander limb bones. *Integr. Comp. Biol.*

Karakasiliotis, K., Schilling, N., Cabelguen, J.-M. and Ijspeert, A. J. (2012). Where are we in understanding salamander locomotion: biological and robotic perspectives on kinematics. *Biol. Cybern* **107**, 529-544. doi:10.1007/s00422-012-0540-4

Kawano, S. M. and Blob, R. W. (2013). Propulsive forces of mudskipper fins and salamander limbs during terrestrial locomotion: implications for the invasion of land. *Integr. Comp. Biol.* **53**, 283-294. doi:10.1093/icb/ict051

Kawano, S. M. and Blob, R. W. (2020). Evaluating limb bone stresses of early tetrapods in the context of the evolutionary invasion of land. *Integr. Comp. Biol.* **60**, E119.

Kawano, S. M., Economy, D. R., Kennedy, M. S., Dean, D. and Blob, R. W. (2016). Comparative limb bone loading in the humerus and femur of the tiger salamander: testing the 'mixed-chain' hypothesis for skeletal safety factors. *J. Exp. Biol.* **219**, 341-353. doi:10.1242/jeb.125799

King, H. M., Shubin, N. H., Coates, M. I. and Hale, M. E. (2011). Behavioral evidence for the evolution of walking and bounding before terrestriality in sarcopterygian fishes. *Proc. Natl. Acad. Sci. U. S. A* **108**, 21146-21151. doi:10.1073/pnas.1118669109

Laurin, M., Girondot, M. and Loth, M.-M. (2004). The evolution of long bone microstructure and lifestyle in lissamphibians. *Paleobiology* **30**, 589-613. doi:10.1666/0094-8373(2004)030<0589:TEOLBM>2.0.CO;2

Laurin, M., Canoville, A. and Germain, D. (2011). Bone microanatomy and lifestyle: A descriptive approach. *Comptes Rendus Palevol.* **10**, 381-402. doi:10.1016/j.crpv.2011.02.003

LeBeau, B., Song, Y. A. and Liu, W. C. (2018). Model misspecification and assumption violations with the linear mixed model: a meta-analysis. *SAGE Open* **8**, 1-16. doi:10.1177/2158244018820380

Lin, D. C., McGowan, C. P., Blum, K. P. and Ting, L. H. (2019). Yank: the time derivative of force is an important biomechanical variable in sensorimotor systems. *J. Exp. Biol.* **222**, jeb180414. doi:10.1242/jeb.180414

Lowell, R. B. (1985). Selection for increased safety factors of biological structures as environmental unpredictability increases. *Science* **228**, 1009-1011. doi:10.1126/science.228.4702.1009

Lüdecke, D., Makowski, D. and Waggoner, P. (2019). *performance: assessment of regression models performance. R package version 0.4.0*. https://CRAN.R-project.org/package=performance.

Martinez, M. M., Full, R. J. and Koehl, M. A. R. (1998). Underwater punting by an intertidal crab: a novel gait revealed by the kinematics of pedestrian locomotion in air versus water. *J. Exp. Biol.* **201**, 2609-2623. doi:10.1242/jeb.201.18.2609

McElroy, E. J., Wilson, R., Biknevicius, A. R. and Reilly, S. M. (2014). A comparative study of single leg ground reaction forces in running lizards. *J. Exp. Biol.* **217**, 735-742. doi:10.1242/jeb.095620

Molnar, J. L. (2021). Variation in articular cartilage thickness among extant salamanders and implications for limb function in stem tetrapods. *Front. Ecol. Evol.* **9**, 671006. doi:10.3389/fevo.2021.671006

Molnar, J. L., Diogo, R., Hutchinson, J. R. and Pierce, S. E. (2020). Evolution of hindlimb muscle anatomy across the tetrapod water-to-land transition, including comparisons with forelimb anatomy. *Anat. Rec.* **303**, 218-234. doi:10.1002/ar.23997

Molnar, J. L., Hutchinson, J. R., Diogo, R., Clack, J. A. and Pierce, S. E. (2021). Evolution of forelimb musculoskeletal function across the fish-to-tetrapod transition. *Sci. Adv.* **7**, eabd7457. doi:10.1126/sciadv.abd7457

Nyakatura, J. A., Andrada, E., Curth, S. and Fischer, M. S. (2014). Bridging "Romer's Gap": limb mechanics of an extant belly-dragging lizard inform debate on tetrapod locomotion during the early Carboniferous. *Evol. Biol.* **41**, 175-190. doi:10.1007/s11692-013-9266-z

Nyakatura, J. A., Melo, K., Horvat, T., Karakasiliotis, K., Allen, V. R., Andikfar, A., Andrada, E., Arnold, P., Lauströer, J., Hutchinson, J. R. et al. (2019). Reverse-engineering the locomotion of a stem amniote. *Nature* **565**, 351-355. doi:10.1038/s41586-018-0851-2

Obst, F. J., Richter, K. and Jacon, U. (1988). *The Completely Illustrated Atlas of Reptiles and Amphibian for the Terrarium*. Neptune City, NJ: T.F.H. publications.

Pace, C. M. and Gibb, A. C. (2014). Sustained periodic terrestrial locomotion in air-breathing fishes. *J. Fish Biol* **84**, 639-660. doi:10.1111/jfb.12318
Petranka, J. W. (1998). *Salamanders of the United States and Canada*. Washington, D.C: Smithsonian Institution Press.
Pierce, S. E., Clack, J. A. and Hutchinson, J. R. (2012). Three-dimensional limb joint mobility in the early tetrapod *Ichthyostega*. *Nature* **486**, 523-526. doi:10.1038/nature11124
Pierce, S. E., Hutchinson, J. R. and Clack, J. A. (2013). Historical perspectives on the evolution of tetrapodomorph movement. *Integr. Comp. Biol.* **53**, 209-223. doi:10.1093/icb/ict022
Pierce, S. E., Lamas, L. P., Pelligand, L., Schilling, N. and Hutchinson, J. R. (2020). Patterns of limb and epaxial muscle activity during walking in the fire salamander, *Salamandra salamandra*. *Integr. Org. Biol* **2**, obaa015. doi:10.1093/iob/obaa015
Reilly, S. M., McElroy, E. J., Andrew Odum, R. and Hornyak, V. A. (2006). Tuataras and salamanders show that walking and running mechanics are ancient features of tetrapod locomotion. *Proc. R. Soc. B Biol. Sci.* **273**, 1563-1568. doi:10.1098/rspb.2006.3489
Rosario, M. V., Sutton, G. P., Patek, S. N. and Sawicki, G. S. (2016). Muscle–spring dynamics in time-limited, elastic movements. *Proc. R. Soc. B Biol. Sci.* **283**, 20161561. doi:10.1098/rspb.2016.1561
Rubin, C. T. and Lanyon, L. E. (1982). Limb mechanics as a function of speed and gait: a study of functional strains in the radius and tibia of horse and dog. *J. Exp. Biol.* **101**, 187-211. doi:10.1242/jeb.101.1.187
Sass, G. G. and Motta, P. J. (2002). The effects of satiation on strike mode and prey capture kinematics in the largemouth bass, *Micropterus salmoides*. *Environ. Biol. Fishes* **65**, 441-454. doi:10.1023/A:1021108519634
Schoch, R. R., Werneburg, R. and Voigt, S. (2020). A Triassic stem-salamander from Kyrgyzstan and the origin of salamanders. *Proc. Natl. Acad. Sci. USA* **117**, 11584-11588. doi:10.1073/pnas.2001424117
Sheffield, K. M. and Blob, R. W. (2011). Loading mechanics of the femur in tiger salamanders (*Ambystoma tigrinum*) during terrestrial locomotion. *J. Exp. Biol.* **214**, 2603-2615. doi:10.1242/jeb.048736
Smith, P. F. (2017). A guerilla guide to common problems in 'neurostatistics': essential statistical topics in neuroscience. *J. Undergrad. Neurosci. Educ.* **16**, R1-R12.
Standen, E. M., Du, T. Y. and Larsson, H. C. E. (2014). Developmental plasticity and the origin of tetrapods. *Nature* **513**, 54-58. doi:10.1038/nature13708
Stokely, P. S. and Holle, P. A. (1954). Appendicular skeleton of the Ambystomidae. *Herpetologica* **10**, 57-61.
Trochet, A., Moulherat, S., Calvez, O., Stevens, V., Clobert, J. and Schmeller, D. (2014). A database of life-history traits of European amphibians. *Biodivers. Data J.* **2**, e4123. doi:10.3897/BDJ.2.e4123
Wainwright, P. C., Mehta, R. S. and Higham, T. E. (2008). Stereotypy, flexibility and coordination: key concepts in behavioral functional morphology. *J. Exp. Biol.* **211**, 3523-3528. doi:10.1242/jeb.007187
Wake, D. B. (2009). What salamanders have taught us about evolution. *Annu. Rev. Ecol. Evol. Syst.* **40**, 333-352. doi:10.1146/annurev.ecolsys.39.110707.173552
Young, V. K. H., Wienands, C. E., Wilburn, B. P. and Blob, R. W. (2017). Humeral loads during swimming and walking in turtles: implications for morphological change during aquatic reinvasions. *J. Exp. Biol.* **220**, 3873-3877.

Supplementary Materials and Methods

Terrestrial force production by the limbs of a semi-aquatic salamander provides insight into the evolution of terrestrial locomotor mechanics

Sandy M. Kawano and Richard W. Blob

Criteria for selecting trials for GRF measurements

Several criteria were used to determine whether a trial was valid for inclusion in our analyses. First, the entire right foot (fore or hind) needed to contact the force plate. Second, any portions of the data that had any body parts other than the limb of interest on the force plate were excluded from analysis. Third, only trials in which the complete limb cycle occurred during movement in a straight path across the force plate were considered (i.e., no turning or walking diagonally relative to the direction of the force plate). Trials were also excluded if the peak net GRF: 1) occurred at 0% or 100% of stance (since those patterns do not necessarily indicate a distinct maximum measurement), or 2) occurred at a time when more than the limb of interest was in contact with the force plate.

Experimental procedures

Data on three-dimensional GRF production of individual limbs walking over level ground were collected using procedures outlined in published studies by Blob and colleagues on fish, amphibians, reptiles, and mammals (Butcher & Blob, 2008; Sheffield & Blob, 2011; Sheffield et al., 2011; Butcher et al., 2011; Kawano & Blob, 2013). Briefly, data on the GRFs imposed on isolated appendages on the right side of the body were recorded (5000 Hz) using a custom-built, multi-axis force plate (K&N Scientific; Guilford, VT, USA) connected to bridge amplifiers. Two digitally synchronized, high-speed cameras (100 Hz; Phantom v.4.1, Vision Research Inc.; Wayne, NJ, USA) simultaneously filmed the dorsal and lateral views, with the dorsal view captured via a mirror positioned over the force plate at an angle of 45° to the trackway (Fig. 1). Data from the high-speed cameras and force plate were synchronized via a trigger that timed the onset of an LED light on the video with the onset of a 1.5 V pulse on the force traces.

GRF production by individual appendages was analyzed during stance, when the foot/fin is in contact with the ground and propulsion is generated. Since some of the force traces did not begin at a baseline of zero Newtons of force, data were padded by mirroring the data at the

beginning and end of the force trace to avoid edge effects during the filtering process. Padded force traces were then filtered using a low-pass, zero phase, second order Butterworth filter with the *signal* package in R (Signal developers, 2013). The order of the polynomial and the cut-off frequency were determined using the signal::buttord() function with the following filter specifications: 2500 Hz frequency, 0.0024 Hz passband frequency, 0.076 Hz stopband frequency, 2 dB passband ripple, and 40 dB stopband attenuation. These frequency values had been normalized to Nyquist frequency to avoid aliasing (Smith, 1997). Padding was removed prior to analysis. Data were then interpolated to 101 points to represent 1% increments, from 0% to 100%, during stance using a cubic spline with the signal::interp1('spline') function.

Filtered data were then used to calculate the magnitude and direction of the GRFs imposed upon the individual limbs during terrestrial locomotion. All force magnitudes were standardized to units of body weight (BW) to account for size differences across individuals and taxa. Magnitudes of the vertical, anteroposterior, and mediolateral components of the GRF were used to calculate the magnitude and orientation of the net GRF vector. Angular orientations were analyzed with respect to vertical (0°): positive values indicated a vector in the anterior or lateral directions and negative values indicated a vector in the posterior or medial directions.

Details on statistical analyses

Handling of data prior to statistical analyses

GRF magnitudes were converted to units of body mass and did not require further conversions to account for size differences among individuals. Angular measurements were also not standardized, as such steps could change the signs of angular values and drastically alter their biological interpretation (e.g., converting the orientation of the GRF from medial to lateral and, thereby, affecting moment arm calculations and estimations of bone loading regimes). Our other variables were continuous, did not include zeros, and did not differ in extreme orders of magnitude (standard errors were close to one or less), so these also were not standardized prior to analyses.

Other common rationales for standardizing data prior to statistical analyses also were not required for our purposes. For example, regression coefficients from the LMMs were not used to predict expected change in response variables for every change in unit of the explanatory variable (i.e., Appendage), so standardization was not necessary. Standardization may be required for models involving interactions (e.g., issues with collinearity can arise with interactions), but our LMMs included only a categorical variable as a fixed effect. Additionally,

since the factor levels within our categorical fixed effect are character strings, they do not contain numerical magnitudes that would weight one group as being more important than the others.

Testing assumptions of the linear mixed effects models (LMMs)

1) Linearity: Since the predictors are categorical, this assumption did not need to be tested.
2) Random sampling: individuals from each species were randomly selected for the study.
3) Normality of the residuals: Residuals were obtained from the LMM output from lme4::lmer() (Bates et al., 2015) and evaluated with Quantile-Quantile (Q-Q) plots using the qqplotr package (Almeida, Loy & Hofmann, 2017) in R.

Major violations of the test assumptions were not found for variables associated with the peak net GRF and yank. Points primarily fell within the confidence band of the Q-Q plot for each variable (Figures S1 – S3), suggesting that these variables reasonably met the assumption of normality. For the variables that showed some deviations from the confidence band, we re-ran the LMMs with the outliers removed (points that were 2x away from the interquartile range of the boxplot) and found that the “outliers” either had no effect on the fixed effects or made only ~4% or less of a difference (Table S1 – S2). At the most extreme, the “outliers” for positive yank in the mediolateral direction for the pelvic appendage decreased the fixed effect 13 – 18%. Thus, the full dataset was used for analysis in the main text since no major violations to the test assumptions were found.

Testing assumptions for peak net GRF data

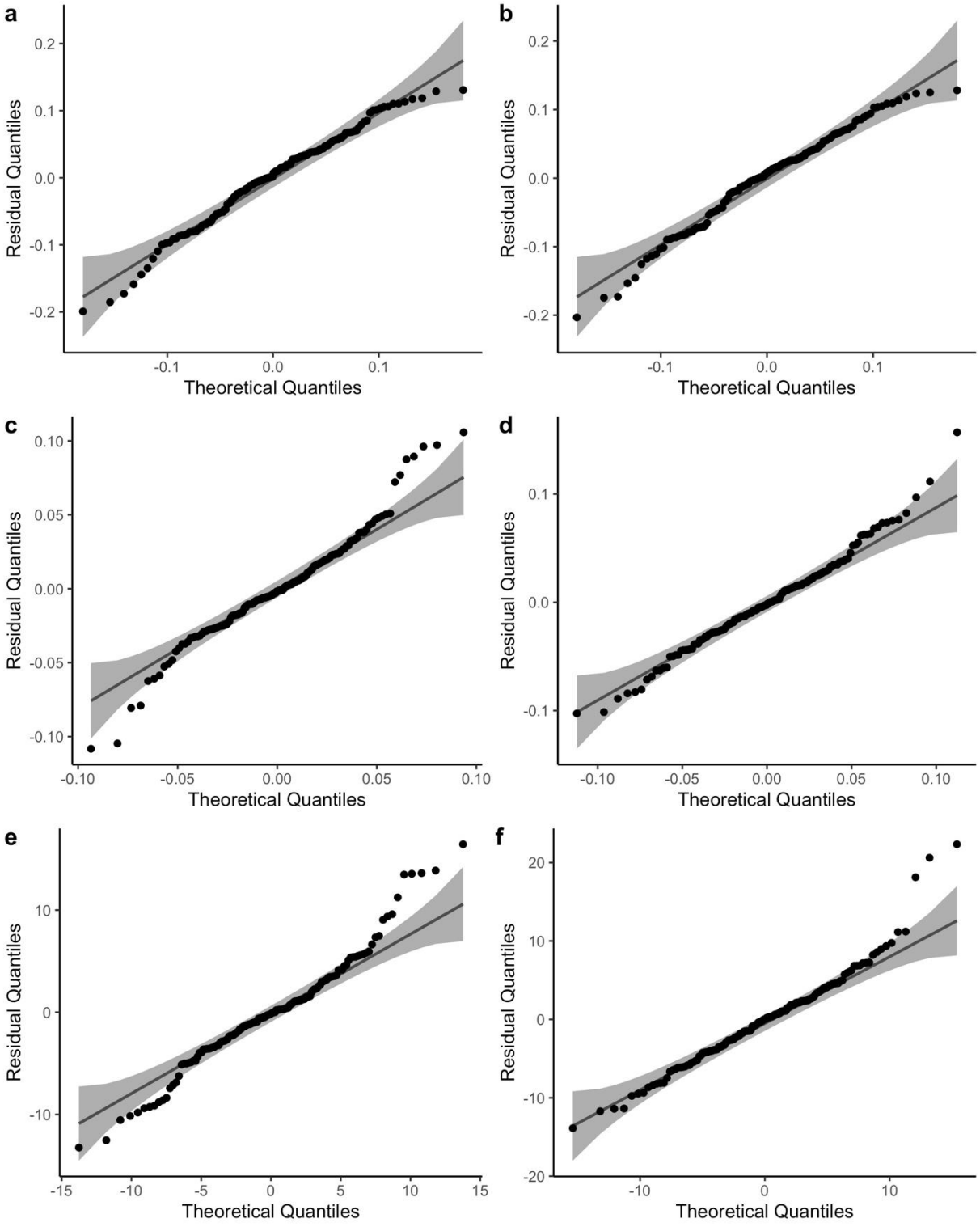

Fig. S1. Graphical assessments of normality in the pectoral LMM (n = 150 trials). The variables include a) net, b) vertical component, c) mediolateral component, d) anteroposterior component, e) mediolateral angle, and f) anteroposterior angle of the GRF. Most of the points fall within the confidence bands of the Q-Q plots for all variables, suggesting that the assumption of normality is reasonably met.

Table S1. Percent differences between the coefficients of the fixed effects produced from the full dataset versus a reduced dataset that has outliers removed for the peak net GRF.

	Full dataset		Dataset with outliers removed		
	FE ± s.e.	**CI**	**FE ± s.e.**	**CI**	**% diff**
Pec - ml					
A. tigrinum	-0.067 ± 0.012	-0.094, -0.041	-0.067 ± 0.0100	-0.089, -0.046	0
P. barbarus	-0.129 ± 0.012	-0.155, -0.102	-0.124 ± 0.0100	-0.149, -0.102	4
P. waltl	-0.087 ± 0.012	-0.114, -0.060	-0.089 ± 0.010	-0.111, -0.066	-2
Pec – ml angle					
A. tigrinum	-8.64 ± 1.36	-11.60, -5.66	-8.64 ± 1.22	-11.30, -5.97	0
P. barbarus	-17.04 ± 1.36	-20.0, -14.06	-16.76 ± 1.22	-19.40, -14.09	2
P. waltl	-13.62 ± 1.40	-16.7, -10.56	-13.91 ± 1.26	-16.70, -11.17	-2
Pec – ap angle					
A. tigrinum	-3.33 ± 1.60	-6.83, 0.16	-3.33 ± 1.71	-7.08, 0.412	0
P. barbarus	6.70 ± 1.64	3.21, 10.20	6.70 ± 1.71	2.96, 10.446	0
P. waltl	-12.38 ± 1.64	-15.95, -8.81	-12.94 ± 1.76	-16.75, -9.123	-4
Pel – ap angle					
A. tigrinum	16.7 ± 2.71	10.39, 22.90	16.1 ± 2.56	10.16, 22.00	4
P. waltl	14.9 ± 2.72	8.59, 21.10	14.9 ± 2.56	8.96, 20.80	0

Testing assumptions for yank data

Maximum yank

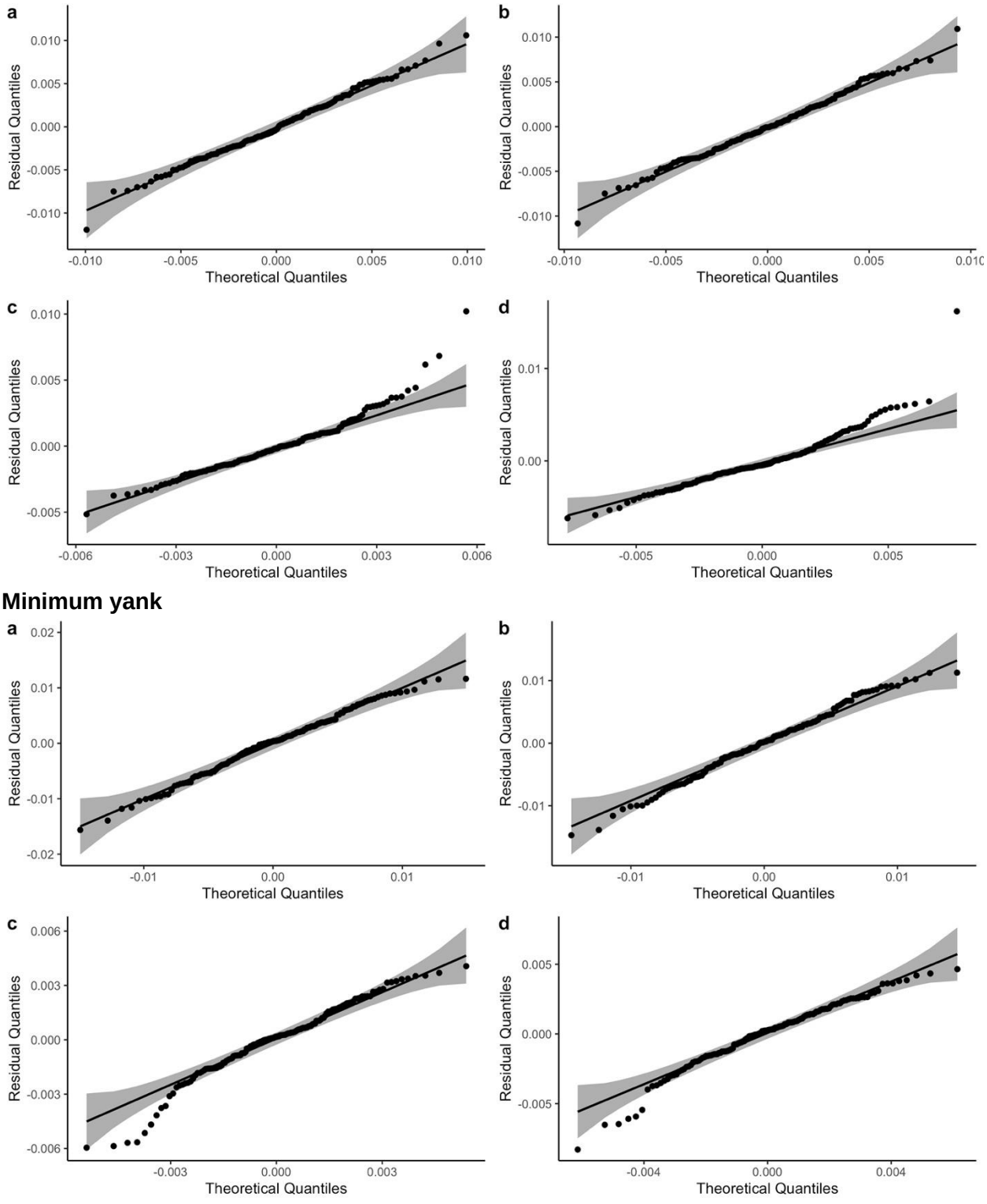

Minimum yank

Fig. S2. QQ plots of maximum and minimum yank values for the a) net, b) vertical component, c) mediolateral component, and d) anteroposterior component of the GRF produced by the pectoral appendages.

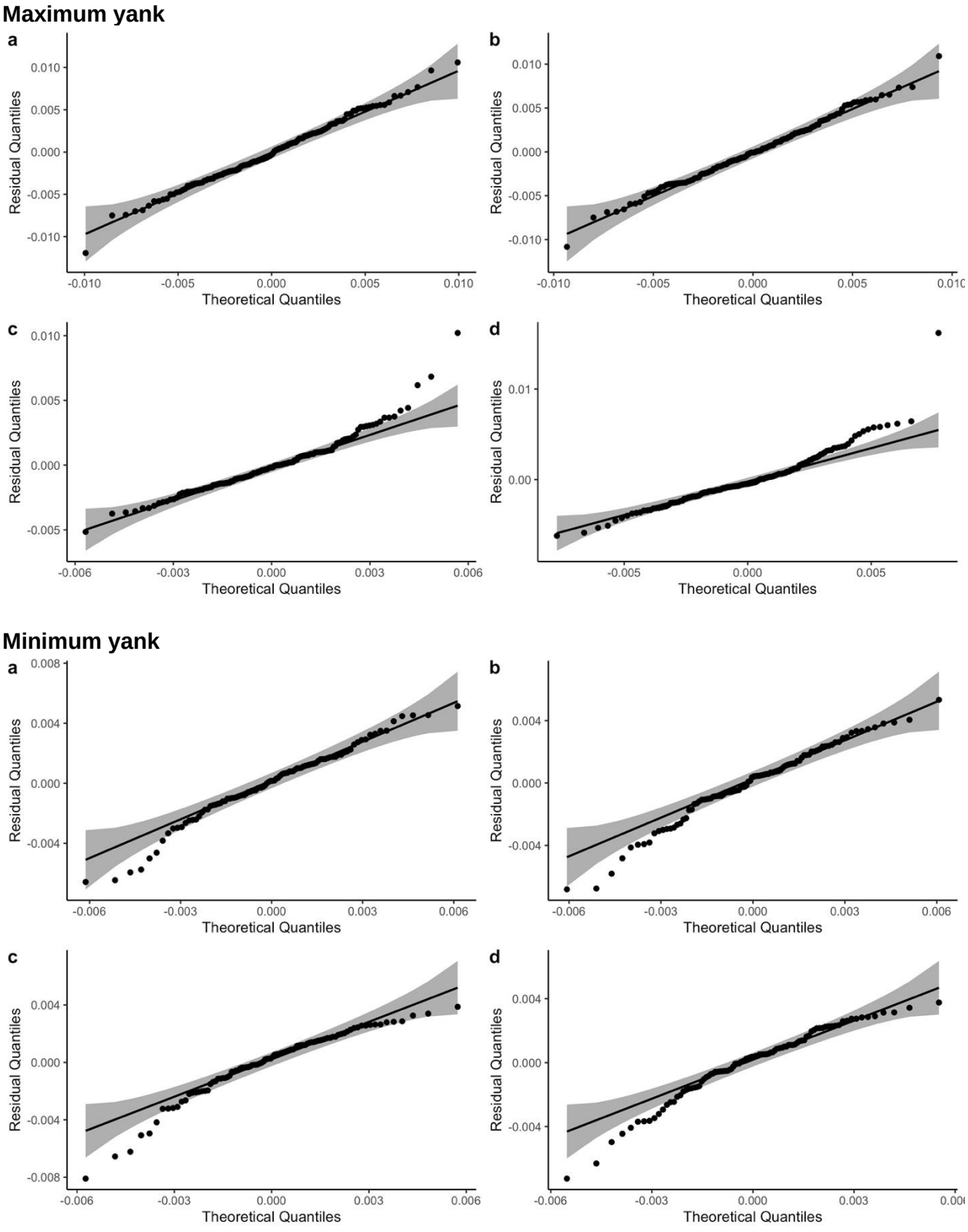

Fig. S3. QQ plots of the maximum and minimum yank values for the a) net, b) vertical component, c) mediolateral component, and d) anteroposterior component of the GRF produced by the pelvic appendages.

Table S2. Percent differences between the coefficients of the fixed effects produced from the full dataset versus a reduced dataset that has outliers removed for the yank data

	Full dataset		Dataset with outliers removed		
	FE ± s.e.	**CI**	**FE ± s.e.**	**CI**	**% diff**
Pec – max - ml					
A. tigrinum	0.0036 ± 0.0007	0.0020, 0.0052	0.0036 ± 0.0006	0.0023, 0.0049	0
P. barbarus	0.0044 ± 0.0007	0.0028, 0.0060	0.0042 ± 0.0006	0.0029, 0.0055	5
P. waltl	0.0060 ± 0.0007	0.0044, 0.0076	0.0058 ± 0.0006	0.0045, 0.0072	3
Pec – max - ap					
A. tigrinum	0.0059 ± 0.0007	0.0044, 0.0075	0.0059 ± 0.0006	0.0046, 0.0073	0
P. barbarus	0.0037 ± 0.0007	0.0022, 0.0053	0.0037 ± 0.0006	0.0024, 0.0051	0
P. waltl	0.0082 ± 0.0007	0.0066, 0.0098	0.0079 ± 0.0006	0.0065, 0.0092	4
Pec – min - ml					
A. tigrinum	-0.0042 ± 0.0006	-0.0056, -0.0028	-0.0041 ± 0.0005	-0.0052, -0.0029	2
P. barbarus	-0.0049 ± 0.0006	-0.0063, -0.0035	-0.0046 ± 0.0005	-0.0058, -0.0035	7
P. waltl	-0.0063 ± 0.0007	-0.0078, -0.0049	-0.0063 ± 0.0005	-0.0075, -0.0051	0
Pec – min – ap					
A. tigrinum	-0.0066 ± 0.0006	-0.0080, -0.0052	-0.0063 ± 0.0006	-0.0075, -0.0051	5
P. barbarus	-0.0039 ± 0.0006	-0.0052, -0.0025	-0.0039 ± 0.0006	-0.0051, -0.0027	0
P. waltl	-0.0045 ± 0.0006	-0.0059, -0.0031	-0.0045 ± 0.0006	-0.0058, -0.0033	0
Pel – max - v					
A. tigrinum	0.0096 ± 0.0013	0.0066, 0.0127	0.0096 ± 0.0013	0.0066, 0.0127	0
P. waltl	0.0052 ± 0.0013	0.0021, 0.0082	0.0047 ± 0.0013	0.0017, 0.0078	11
Pel – max - ap					
A. tigrinum	0.0087 ± 0.0009	0.0067, 0.0107	0.0077 ± 0.0006	0.0064, 0.0090	13
P. waltl	0.0060 ± 0.0009	0.0040, 0.0080	0.0051 ± 0.0006	0.0038, 0.0065	18
Pel – max - net					
A. tigrinum	0.0105 ± 0.0013	0.0074, 0.0135	0.0105 ± 0.0014	0.0074, 0.0136	0
P. waltl	0.0058 ± 0.0013	0.0027, 0.0088	0.0055 ± 0.0014	0.0023, 0.0086	7
Pel – min – ml					
A. tigrinum	-0.0042 ± 0.0004	-0.0052, -0.0033	-0.0041 ± 0.0004	-0.0050, -0.0032	2
P. waltl	-0.0044 ± 0.0004	-0.0053, -0.0034	-0.0042 ± 0.0004	-0.0051, -0.0033	5
Pel – min – ap					
A. tigrinum	-0.0070 ± 0.0006	-0.0083, -0.0057	-0.0068 ± 0.0005	-0.0078, -0.0057	3
P. waltl	-0.0061 ± 0.0006	-0.0074, -0.0048	-0.0061 ± 0.0005	-0.0072, -0.0050	0

Comparison of stance durations

When we ran a species x stance duration interaction term as a fixed effect in our LMMs, stance duration was a good predictor in only the anteroposterior component and angle of the GRF for the pectoral appendages. The interaction between *P. barbarus* and stance duration was important for the mediolateral component, anteroposterior component, and anteroposterior angle of the GRF, so we report results for these comparisons as well. Comparisons of the point estimates for the species between our reduced and full models indicated that including stance duration in our LMMs had minimal to no effect for almost all variables (Table S3). Point estimates between the reduced and full models differed by less than 2 degrees for the mediolateral and anteroposterior angles of the GRF but had overlapping confidence intervals, suggesting these differences were negligible (Table S3). The mediolateral components of the GRF were equivalent between the reduced and full models for the salamanders but was 0.019 BW lower in the full model for *P. barbarus*, which only strengthened one of the main findings in our study. The anteroposterior component of the GRF had the most pronounced differences between the reduced and full models but did not affect the main patterns found in our results. Salamander forelimbs became slightly (10 – 20 %) more deceleratory and mudskipper pectoral fins became moderately less acceleratory (25%).

Table S3. Comparison of locomotor variables between the pectoral appendages of mudskippers and salamanders at the peak net GRF with and without stance duration as a fixed effect

	Periophthalmus barbarus n = 50		*Pleurodeles waltl* n = 50		*Ambystoma tigrinum* n = 50	
	FE ± s.e.	CI	FE ± s.e.	CI	FE ± s.e.	CI
Net GRF (BW)						
Excluding stance duration	0.443 ± 0.014	0.412, 0.473	0.404 ± 0.015	0.372, 0.436	0.458 ± 0.014	0.427, 0.488
Including stance duration	0.448 ± 0.018	0.410, 0.486	0.407 ± 0.016	0.372, 0.442	0.462 ± 0.015	0.429, 0.495
Vertical GRF (BW)						
Excluding stance duration	0.417 ± 0.012	0.392, 0.442	0.381 ± 0.012	0.355, 0.407	0.447 ± 0.012	0.422, 0.473
Including stance duration	0.411 ± 0.013	0.383, 0.439	0.384 ± 0.013	0.356, 0.412	0.450 ± 0.012	0.423, 0.476
Mediolateral GRF (BW)						
Excluding stance duration	-0.129 ± 0.012	-0.115, -0.102	-0.087 ± 0.013	-0.114, -0.060	-0.067 ± 0.012	-0.094, -0.041
Including stance duration	-0.148 ± 0.013	-0.176, -0.120	-0.086 ± 0.012	-0.112, -0.059	-0.067 ± 0.012	-0.093, -0.041
Anteroposterior GRF (BW)						
Excluding stance duration	0.048 ± 0.013	0.020, 0.076	-0.086 ± 0.013	-0.115, -0.057	-0.029 ± 0.013	-0.058, -0.001
Including stance duration	0.036 ± 0.014	0.006, 0.066	-0.095 ± 0.013	-0.124, -0.066	-0.035 ± 0.013	-0.063, -0.007
Mediolateral angle (°)						
Excluding stance duration	-17.04 ± 1.36	-20.00, -14.06	-13.62 ± 0.140	-16.70, -10.56	-8.64 ± 1.36	-11.60, -5.66
Including stance duration	-17.91 ± 1.47	-21.10, -14.74	-13.13 ± 1.47	-16.30, -9.93	-8.29 ± 1.43	-11.40, -5.18
Anteroposterior angle (°)						
Excluding stance duration	6.70 ± 1.60	3.21, 10.20	-12.38 ± 1.64	-15.95, -8.81	-3.33 ± 1.60	-6.83, 0.16
Including stance duration	5.09 ± 1.70	1.53, 8.65	-13.64 ± 1.56	-17.00, -10.28	-4.23 ± 1.49	-7.48, -0.99

Statistical analyses were based on the model: lmer(y ~ Species + (1|Individual), REML=True) when excluding stance duration or lmer(y ~ Species*stance_s + (1|Individual), REML=True) when including stance duration. Fixed effect (FE) values, standard errors, and confidence interval (CI) were estimated from the linear mixed effects model using the emmeans R package. The interaction between species and stance duration was evaluated at the average stance duration (0.487 secs). $R^2_{LMM(m)}$ represents the variance explained by the fixed effects whereas $R^2_{LMM(c)}$ represents the variance explained by the combination of fixed and random effects, and were calculated using the performance::r2_nakagawa() function in R.

REFERENCES

Almeida A, Loy A, Hofmann H. 2017. *qqplotr: Quantile-Quantile Plot Extensions for "ggplot2". R package version 0.0.3 initially funded by Google Summer of Code 2017. https://github.com/aloy/qqplotr.*

Ashley-Ross MA. 1994. Hindlimb kinematics during terrestrial locomotion in the salamander (*Dicamptodon tenebrosus*). *Journal of Experimental Biology* 193:285–305.

Ashley-Ross MA, Barker JU. 2002. The effect of fiber-type heterogeneity on optimized work and power output of hindlimb muscles of the salamander Ambystoma tigrinum. *Journal of Comparative Physiology A* 188:611–620. DOI: 10.1007/s00359-002-0336-4.

Ashley-Ross MA, Lundin R, Johnson KL. 2009. Kinematics of level terrestrial and underwater walking in the California newt, *Taricha torosa*. *Journal of Experimental Zoology* 311A:240–257. DOI: 10.1002/jez.522.

Bates D, Maechler M, Bolker B, Walker S. 2015. Fitting linear mixed-effects models using lme4. *Journal of Statistical Software* 67:1–48. DOI: doi:10.18637/jss.v067.i01.

Bennett AF, Garland T, Else PL. 1989. Individual correlation of morphology, muscle mechanics, and locomotion in a salamander. *The American journal of physiology* 256:1200–1208.

Butcher MT, Blob RW. 2008. Mechanics of limb bone loading during terrestrial locomotion in river cooter turtles (*Pseudemys concinna*). *The Journal of experimental biology* 211:1187–1202. DOI: 10.1242/jeb.012989.

Butcher MT, White BJ, Hudzik NB, Gosnell WC, Parrish JHA, Blob RW. 2011. In vivo strains in the femur of the Virginia opossum (*Didelphis virginiana*) during terrestrial locomotion: testing hypotheses of evolutionary shifts in mammalian bone loading and design. *The Journal of experimental biology* 214:2631–2640. DOI: 10.1242/jeb.049544.

Canoville A, Laurin M. 2009. Microanatomical diversity of the humerus and lifestyle in lissamphibians. *Acta Zoologica* 90:110–122. DOI: 10.1111/j.1463-6395.2008.00328.x.

Deban SM, Schilling N. 2009. Activity of trunk muscles during aquatic and terrestrial locomotion in *Ambystoma maculatum*. *The Journal of experimental biology* 212:2949–59. DOI: 10.1242/jeb.032961.

Delvolvé I, Bem T, Cabelguen JM. 1997. Epaxial and limb muscle activity during swimming and terrestrial stepping in the adult newt, *Pleurodeles waltl*. *Journal of neurophysiology* 78:638–50.

Karakasiliotis K, Schilling N, Cabelguen J-M, Ijspeert AJ. 2012. Where are we in understanding salamander locomotion: biological and robotic perspectives on kinematics. *Biological Cybernetics* 107:529–544. DOI: 10.1007/s00422-012-0540-4.

Kawano SM, Blob RW. 2013. Propulsive forces of mudskipper fins and salamander limbs during terrestrial locomotion: implications for the invasion of land. *Integrative and comparative biology* 53:283–294. DOI: 10.1093/icb/ict051.

Laurin M, Girondot M, Loth M-M. 2004. The evolution of long bone microstructure and lifestyle in lissamphibians. *Paleobiology* 30:589–613.

Obst FJ, Richter K, Jacon U. 1988. *The completely illustrated atlas of reptiles and amphibian for the terrarium*. Neptune City, NJ: T.F.H. publications.

Petranka JW. 1998. *Salamanders of the United States and Canada*. Washington, D.C.: Smithsonian Institution Press.

Pierce SE, Hutchinson JR, Clack JA. 2013. Historical perspectives on the evolution of tetrapodomorph movement. *Integrative and Comparative Biology* 53:209–23. DOI: 10.1093/icb/ict022.

Sheffield KM, Blob RW. 2011. Loading mechanics of the femur in tiger salamanders (*Ambystoma tigrinum*) during terrestrial locomotion. *Journal of Experimental Biology* 214:2603–2615. DOI: 10.1242/jeb.048736.

Sheffield KM, Butcher MT, Shugart SK, Gander JC, Blob RW. 2011. Locomotor loading mechanics in the hindlimbs of tegu lizards (*Tupinambis merianae*): comparative and evolutionary implications. *Journal of Experimental Biology* 214:2616–2630. DOI: 10.1242/jeb.048801.

Signal developers. 2013.signal: Signal processing. *Available at http://r-forge.r-project.org/projects/signal/.*

Smith S. 1997. *The scientist and engineer's guide to digital signal processing*. San Diego, CA: California Technical Publishing.

Stokely PS, Holle PA. 1954. Appendicular skeleton of the Ambystomidae. *Herpetologica* 10:57–61.

Wake DB. 2009. What salamanders have taught us about evolution. *Annual Review of Ecology, Evolution, and Systematics* 40:333–352. DOI: 10.1146/annurev.ecolsys.39.110707.173552.